



Liquefaction hazard assessment in a seismically active region of Himalayas using geotechnical and geophysical investigations: a case study of the Jammu Region

Abdullah Ansari¹ · Falak Zahoor^{1,2} · Kondalamahanaty Seshagiri Rao¹ · Arvind Kumar Jain¹

Received: 4 April 2022 / Accepted: 26 July 2022 / Published online: 4 August 2022
© Springer-Verlag GmbH Germany, part of Springer Nature 2022

Abstract

The Jammu Region (JR) in the northwestern Himalayas triggered by medium to high magnitude near-field as well as far-field earthquake events, including the most recent 2019 Mirpur earthquake. In this paper, an attempt has been made to develop the zonation map for liquefaction hazard in the JR based on liquefaction potential index (LPI) and probability of liquefaction (P_L). To achieve this, factor of safety against liquefaction was estimated using standard penetration test (SPT) data collected from geotechnical consultancies and shear wave velocity measured during field testing at 243 locations, and an integrated liquefaction hazard map generated. The liquefaction features such as sand blows and ground rupture were found in Jatah (Samba district) and Simbal (Jammu district). According to the integrated hazard map, places near the bank of Tawi River and Ravi River in Jammu have young alluvium, making them particularly prone to liquefaction. Liquefaction does not occur in the eastern and western sections because of high shear wave velocities and rock at shallow depth, and it also does not occur in the central area due to thick sand deposits. LPI values ranged from 0 to 27.45 having very low to very high liquefaction risk. P_L is greater than 0.75 for sites located on the southwestern side due to uniformly graded soil having extremely low SPT (N) and V_s values. This study will aid site planners in the construction of structures that consider liquefaction mitigation and well-defined liquefaction risk measures.

Keywords Liquefaction potential index · Liquefaction hazard map · Standard penetration test · Shear wave velocity · Jammu and Kashmir

Introduction

The Jammu and Kashmir region in northern India has witnessed several natural disasters like earthquakes, floods, landslides, and avalanches (Sana 2019; Ansari et al. 2021a, b). The continuing collision of the Indian and Eurasian plates has resulted in earthquakes of varying magnitudes in the Himalayan region including the deadliest Muzaffarabad earthquake (M_w 7.6) in 2005 and the most recent Mirpur earthquake (M_w 5.6) in 2019 (Ansari et al. 2022d; Gupta and Satyam

2022). The 2005 Muzaffarabad earthquake resulted in severe damage in Muzaffarabad, Uri, Kupwara, and Balakot causing the deaths of 72,763 people and injuring a further one lakh people (Sana and Nath 2016; Ansari et al. 2017; Sana 2019; Sana et al. 2019; Powali et al. 2020). The tremors of the 2019 Mirpur earthquake in Pakistan were felt in the Jammu Region (JR), Punjab region, Uttarakhand, and Delhi causing the deaths of 50 people and property damage in small towns of Jatlan, Manda, and Afzalpur near Mirpur city. The slope failure and ground shaking were observed in the Rajouri and Poonch districts due to the 2019 Mirpur earthquake. The post-effect of these earthquake events created the problem of liquefaction in different parts of Jammu and Kashmir (Ansari et al. 2022b). The consequently induced acceleration and internal strains may generate higher in situ shear stress along a potential failure line during earthquakes (Papathanassiou 2008; Zhan and Kanamori 2016). Furthermore, as a result of the ground shaking, the material may tend to densify, resulting in increased pore pressure in saturated loose soil and,

✉ Abdullah Ansari
aamomin183@gmail.com; ansariaa@civil.iitd.ac.in

¹ Department of Civil Engineering, Indian Institute of Technology Delhi, Hauz Khas, New Delhi 110016, India

² Department of Civil Engineering, National Institute of Technology Srinagar, Jammu and Kashmir 190006, Srinagar, India

as a result, a reduction in effective stresses. Liquefaction of soils occurs when a significant extra pore pressure builds up due to partially undrained deformation of loose soils, resulting in a lower undrained shear strength than drained shear strength. In general, each site's liquefaction threat is assessed using a factor of safety (F_s) based on the cyclic stress and resistance concept, and liquefaction potential index (LPI). The sites with $F_s < 1$ are regarded as liquefiable, while those with $F_s > 1$ are considered as non-liquefiable. $F_s = 1$ denotes the limiting equilibrium state.

Over the last few years, construction of mega projects including the world's tallest Chenab bridge, India's first cable-stayed Anji Khad bridge, Pir Panjal tunnel, and Udhampur Srinagar Baramulla Rail Link Project (USBRL) have progressed at a faster rate in the JR (Ansari et al. 2022a, b, c, d, e). The past historical records of the earthquake events and rapid infrastructural development push to assess the liquefaction hazard of the study area. In the present study, an attempt has been made to provide the liquefaction hazard maps in terms of F_s against liquefaction, liquefaction potential index (LPI), and probability of liquefaction (P_L) at different depths for the JR based on geotechnical and geophysical approaches. The standard penetration test (SPT) and cone penetration test (CPT) are the most common method used to calculate cyclic resistance. The Seismic Dilatometer Marchetti Test (SDMT) is increasingly becoming more widely used in normal geotechnical investigations, allowing for the collection of a large number of data points. The SDMT calculates a horizontal stress index that has a strong link to soil liquefaction (Grasso and Maugeri 2008; Grasso et al. 2020).

The liquefaction hazard assessment is carried out using both SPT (Boulanger and Idriss 2014) and shear wave velocity (V_s)-based methods (Andrus and Stokoe 2000; Andrus et al. 2004). Extensive borehole data have been collected from geotechnical consultancies for the study area. The geophysical tests were conducted on natural land to examine the subsurface data for shear wave velocity at different depths based on the multichannel analysis of surface wave (MASW) technique. The ground rupture was observed during the field investigation in the Simbal village in the JR. Local people of Jatah (Samba district) observed sand blows near Degh Nala after the 2019 Mirpur earthquake. The liquefaction potential of the study area was assessed using the PGA at the surface level from seismic response analysis in DEEPSOIL (Hashash et al. 2008), geotechnical data from consultancies, and geophysical data from field tests at 243 site locations. Based on the possibility of liquefaction, the study area is classified into different zones using geotechnical, geophysical, and seismic response data.

The areas in the southern part of Jammu, Samba, and Kathua have been identified as liquefiable due to the existence of silty sand and fine sand, as well as a shallow water table.

The sites in the northern districts like Ramban and Poonch, and the northeastern part of Doda and Kishtwar are not susceptible to liquefaction. An integrated liquefaction hazard map for the study area is also generated using the findings of both SPT- and V_s -based techniques. It has been also reported that a few locations that are prone to liquefaction using a V_s -based approach is not susceptible to liquefaction using SPT-based approach. The maps for liquefaction potential index (LPI) and probability of liquefaction (P_L) is also presented, which gives a better delineation of hazards in the study area. This data may be used as a tool for engineers to make risk-based design decisions for liquefaction mitigation in the study area.

Tectonics and local geology of the study area

The JR in the northwestern Himalayas is limited on the north by Kashmir valley and on the east by Ladakh, where the southwestern part has flat terrain, and the rest is made up of Jammu hills (Ansari et al. 2022a). The height of the Jammu hills ranges from 330 m in the Jammu city to 1638 m in the Kishtwar on the eastern side, which touches Ladakh on the India-China border (Paul et al. 2018; Pandita et al. 2019). The groundwater table depth varies between 2 and 22 m, with north to south flow, due to variations in subsurface condition and topographical changes from Reasi in the north to Kathua in the south (Bhanja et al. 2018; CGWB 2020; Qadir et al. 2020). The Chenab, Tawi, and Ravi are the main rivers flowing in the JR, which further enters the territory of Pakistan. The Chandra and Bhaga rivers, which meet near Keylong in Himachal Pradesh to form the Chandra-Bhaga or Chenab River, are two important tributaries of the Chenab River. After passing through the Kashmir Himalayas, the river emerges into the plains near Akhnour in Jammu. The southern portions of Samba and Kathua, near Pathankot in Punjab fall under the basin of the Ravi River (Razzia and Dar 2021). The Tawi River passes through the Doda, Udhampur, and Jammu and then merges with the Chenab River near Sialkot in Pakistan.

The Jammu, Samba, Kathua, and southwestern part of Udhampur districts lie at the foothills of Siwalik, built over deep sedimentary basins made up of unconsolidated quaternary sediments of the Jammu formation, older and younger alluvium (Ansari et al. 2021a). Subsurface strata from Jammu to Reasi show Dolomite formation and Murre formation (Tiwari and Latha 2020). The northern part of Jammu city comprises of Nagrota formation while the southern part consists of younger alluvium near the banks of the Tawi River. On the western side of Udhampur, clast-supported deposits can be found at the top of the fan, sandy deposits can be found in the central area, and clay deposits within gravel bands can be found at the bottom of the fan (Mahajan et al. 2012). Because of its extensively weathered and fractured

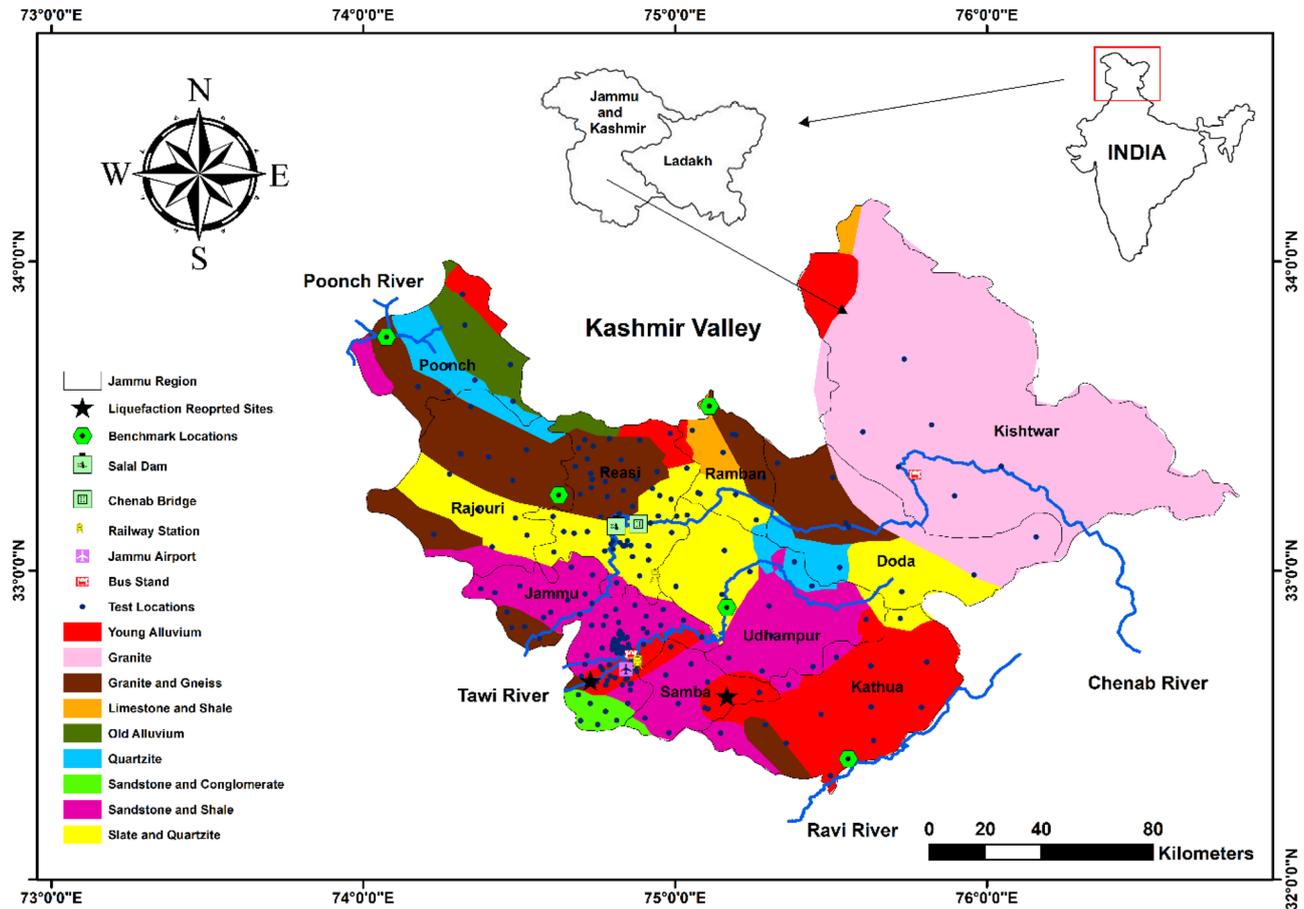


Fig. 1 Lithology map of the Jammu Region with benchmark locations and sites where liquefaction was observed during far-field earthquakes

character, dolomite rock formation regions are the most predominant among the primary rock types found in the study area. The thickness of dolomite ranges from 150 to 200 m (Srinivas et al. 2014). The geographical location of the study area along with lithological formations is presented in Fig. 1.

The JR has been impacted due to the near-field as well as far-field earthquakes in the Himalayan region extending up to Hindukush in Afghanistan (Lister et al. 2008; Asim et al. 2017). The

major earthquake events in the northwestern Himalayas are listed in Table 1. The following Fig. 2 presents the total number of earthquake events that occurred in and around the JR for different magnitude classes in the last 500 years. The Jhelum Fault (JF), Attock Fault (AF), Reasi Fault (RF), Balakot-Bagh Fault (BBF), Deosai Fault (DF), Jwalamukhi Thrust Jwalamukhi Thrust Hanna Fault (HF), Batal Fault (BF), and Mawer Fault (MF) are few of the active faults that surround this area (Bilham and

Table 1 Damage and casualties caused due to historical earthquakes around the Jammu Region in the northwestern Himalayas

Latitude	Longitude	Depth (km)	M_w	Location	Damage and casualties	Year
33.5° N	75.50° E	10	7.6	Kashmir	60,000 dead	1555
33.90° N	72.30° E	10	6.5	Islamabad (Pakistan)	32,000 dead	1669
34.10° N	74.80° E	20	7	Jammu and Kashmir	3500 dead; 75,000 huts destroyed (Ahmad et al. 2014)	1885
34.49° N	73.15° E	10	7.6	Muzaffarabad (Pakistan)	72,763 dead; 75,266 injured; more than one lakh buildings and houses partially or completely collapsed, liquefaction features observed in Jammu (Simbal) and Kupwara (Malik et al. 2007; Jayangondapeumal et al. 2008; Sana and Nath 2016)	2005
36.4° N	70.86° E	213	7.5	Hindukush (Afghanistan)	399 dead; 2678 injured; damage to more than one lakh buildings	2015
33.11° N	73.77° E	10	5.6	Mirpur (Pakistan)	50 dead; 1000 injured; road and bridge damage in Jatlan and Manda, liquefaction features observed in Jatah (Samba district)	2019

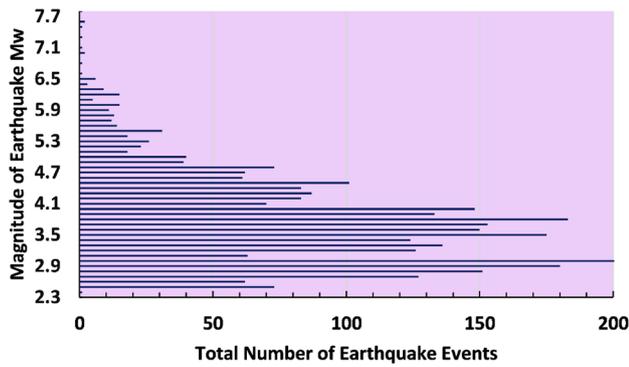


Fig. 2 Total number of earthquake events that occurred in the north-western Himalayas in the last 500 years (1521 AD to 2021 AD)

Wallace 2005). The Main Central Thrust (MCT) distinguishes the crystalline rocks of the higher Himalayas from the formations of the lower Himalayas (Gupta and Gahalaut 2014). Along the

JR's northern boundary, the Main Boundary Thrust (MBT) and Panjal Thrust (PT) run parallel. NNW-SSE and NW-SE trends are shown by the Jwalamukhi Thrust (JT) and Balapur Thrust (BT) respectively (Malik and Mohanty 2007; Alam et al. 2015; Sana and Nath 2017). The NE-dipping Kishtwar Fault (KF) and the NS-trending Jhelum Fault (JF) are the two major local strike-slip faults in the JR. The BBF, which is NE dipping in Pakistan, is the primary cause of the 2005 Muzaffarabad earthquake (Avouac et al. 2006; Pathier et al. 2006). Active Reasi Fault (RF) and Udhampur Fault (UF) pass through the core center section of the JR in addition to the MBT. As a result of the imbrication of the lower Himalayas into a deeper structural level, the Kishtwar Window (KW) developed inside the crystalline upper Himalayas (Singh 2010; Pandey et al. 2017; Pandita et al. 2021). In 2013, an earthquake of a magnitude of M_w 5.7 struck Kishtwar, with the epicenter 258 km from Jammu. The major tectonic features along with earthquake epicenters having magnitude $M_w \geq 4.1$ are shown in the following Fig. 3.

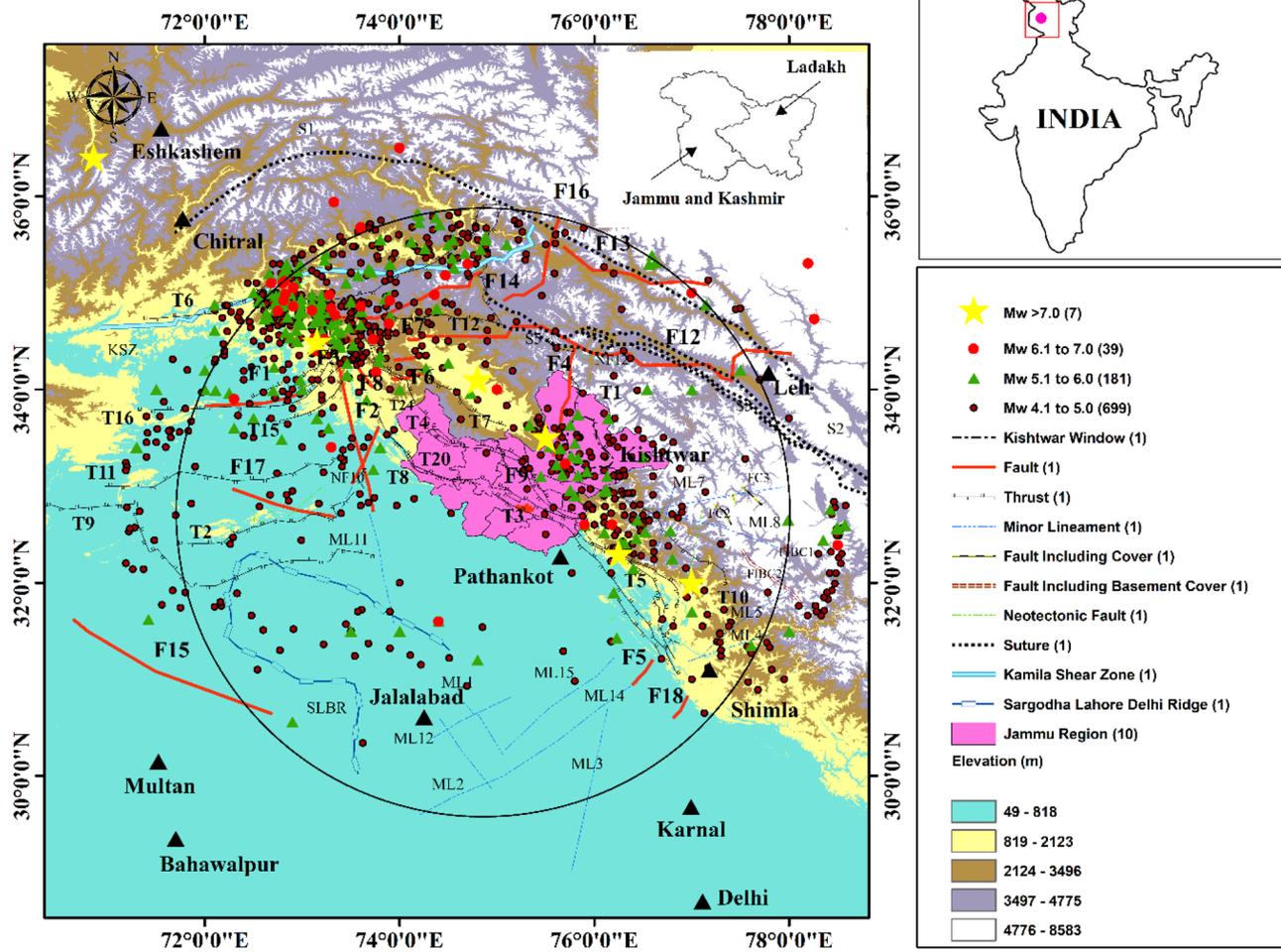


Fig. 3 Seismotectonic map of the Jammu Region and surroundings presenting major tectonic features and epicenter of earthquake events with magnitude, $M_w \geq 4.1$

Post-earthquake effects reported during field investigation

The epicenters of the 2005 Muzaffarabad earthquake and the 2019 Mirpur earthquake are located around 232 and 122 km from Jammu (Fig. 4a). Jayangondapeumal et al. (2008) reported the well-developed liquefaction features at Simbal village near Jammu airport. Open cracks and sand blow on the ground owing to intense motion observed as liquefaction evidence. Through longitudinal fissures, the sand vented water to the ground surface (Rai and Murty 2006; Malik et al. 2007). In May to June 2021, a field survey in the Jatah village, which is next to Degh Nala in the JR's Samba district. During the 2019 earthquake near Mirpur, a few villagers in Jatah village on the Indo-Gangetic Plain felt strong triggering and noticed the swaying of electric poles. Due to the shaking effect of the far-field earthquake, this event caused a shift in the water table. Local residents observed sand blows at three locations as evidence of liquefaction caused by the far-field earthquake, which had an epicenter in Mirpur, 137 km away. As shown in the following Fig. 4c, the largest sand blows appeared on the east side of Degh Nala. In Simbal, a 20-m long ground rupture was identified, which is created due to strong motions during the 2019 Mirpur earthquake (Fig. 4b). The observed liquefaction characteristics for these two sites which are located at a far distance from the epicenter of both the 2005 Muzaffarabad earthquake and

2019 Mirpur is due to dynamic stress transmission inside the subsurface strata. If the soil has previously liquefied as a result of an earthquake, it may do so again in future earthquake events. Prior seismic strain history has a major impact on the resistance of soils to liquefaction phenomena.

Geotechnical, geophysical, and ground response investigation

For a detailed assessment of liquefaction susceptibility of any area in an earthquake-prone zone, subsurface soil data is very important to proceed with the analysis. For this purpose, subsurface geotechnical data is collected from geotechnical consultancies working on different projects related to infrastructure and town planning in Jammu and Kashmir. The standard penetration test (SPT) gives an idea about the N value, density, and plasticity index at different depths for a borehole at a particular site of interest to reflect the penetration resistance (Satyam 2006; Rao and Satyam 2007; Thaker and Rao 2014; Naik and Patra 2018). The soils in the southern sections of Jammu, Samba, and Kathua are generally clayey to clayey silt in the top few meters, followed by sands, and silty sands. The shear wave velocity (V_s) is associated with the stiffness of soil deposits showing the overall behavior of soil under seismic conditions (Trivedi et al. 2009). For this purpose, the multichannel analysis of surface

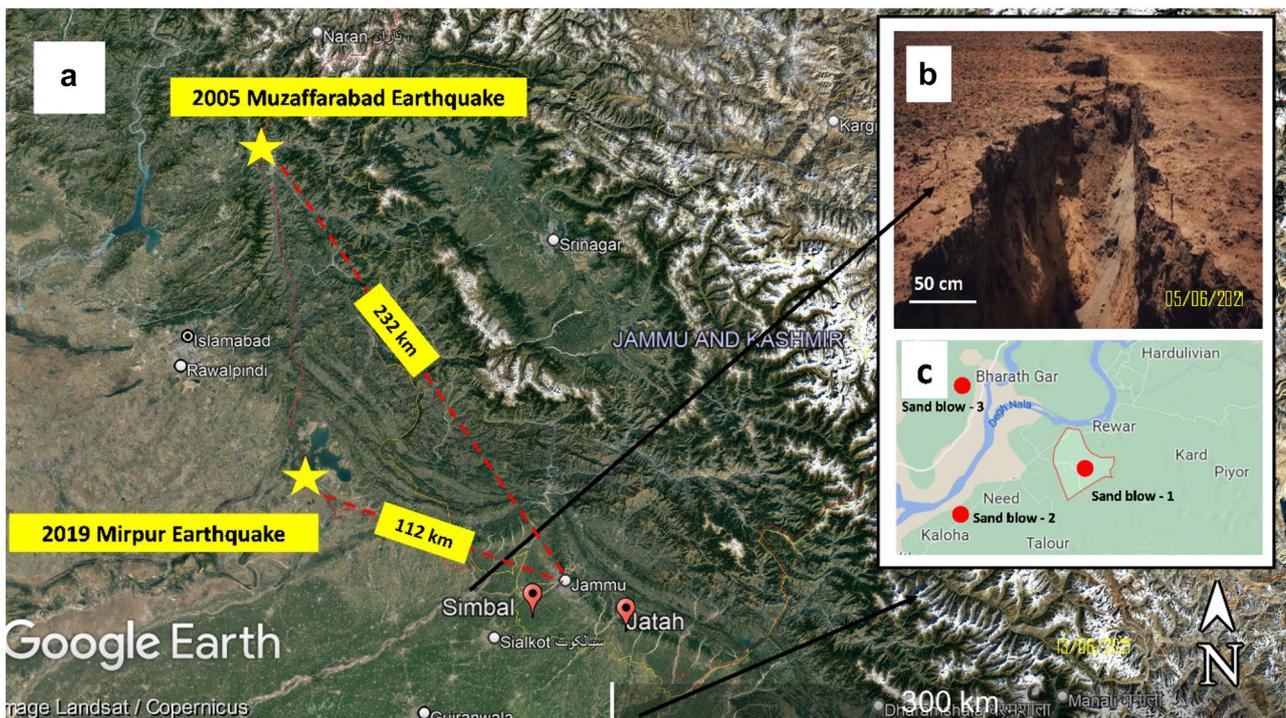


Fig. 4 Liquefaction features observed in the Jammu Region (Jammu and Kashmir) during the field survey after the 2019 Mirpur earthquake. **a** Location map, **b** ground rupture at Simbal in Jammu, and **c** sand blows near Degh Nala in Jatah village in Samba

waves (MASW) method (Park et al. 1999, 2001; Rix et al. 2001; Satyam and Rao 2008; Naik et al. 2021) was used to get a high resolution of subsurface strata at shallow depth. Geophysical approaches have been used in the past to check the susceptibility of sites for liquefaction in tectonically active areas (Park et al. 2002; Yilmaz et al. 2006; Karastathis et al. 2010; Rathod 2011; Rao and Rathod 2014; Satyam and Rao 2014). The geophysical field testing was performed at 243 locations to cover the whole study area using Tromino (Micromed s.p.a. 2009) provided by the Geotechnical Division of National Institute of Technology Srinagar, Jammu and Kashmir, having a frequency range of 0.1–1024 Hz. The testing locations are marked in the map presented in Fig. 1. The recorded data is analyzed to produce Rayleigh wave dispersion curves, which essentially show how the phase velocity of seismic waves in the shallow subsurface changes with frequency. The average shear wave velocity (V_{s30}) is calculated for the top 30 m which ranges between 185 m/s on the southern side to 935 m/s on the northern side of the JR.

Depth-wise variation of shear wave velocity (V_s) and SPT (N) values are presented in Fig. 5. Although it is preferred to establish the shear wave velocity directly from field experiments, doing so at all site locations is generally not cost-effective. Various empirical relationships for determining shear wave velocity using SPT (N) values are known for the Indo-Gangetic area (Rao and Rathod 2014; Naik and Patra 2018). The geotechnical parameters obtained from consultancies and V_s data obtained from geophysical field testing were integrated for the study region to generate a correlation for all types of soils using regression analysis, as follows:

$$V_s = 211.44 N^{0.2862} \tag{1}$$

The shear wave and other dynamic soil profiles of the JR can be characterized using the proposed empirical correlation between shear wave velocity and SPT blow counts. The primary soil type in the southwestern part of the study region is sandy silt or silty sand. The performance of the

suggested correlation is evaluated by comparing it to the shear wave velocity (V_s) recorded during geophysical testing. The proposed Eq. (1) better fits the majority of the data for shear wave velocity estimated for examined soils. The existence of mechanically unstable soil formations was shown by the delineated clay and peat within the typical foundation depth.

For any site of interest, seismic waves transmitted through a soil layer maybe get amplified or deamplified as compared to bedrock motion. This effect can be studied by considering local site effects to understand the seismic response of soil deposits. Local site effect and extensive site characterization are necessary for places where shallow geology is diverse and strong topographic fluctuations prevail (Bonilla et al. 1997; Nardone and Maresca 2011; Singh et al. 2017; Ferraro et al. 2018; Putti and Satyam 2018; Naik et al. 2020).

In this study, input bedrock motion recorded at nine different seismic stations located in the central, north-western, and northeastern Himalayas were considered and one-dimensional seismic response analysis for the equivalent linear case has been done using DEEPSOIL (Hashash et al. 2008; Thaker et al. 2012; Jishnu et al. 2013) at all sites where geophysical field testing was carried out within the study area. The bedrock PGA of 0.24 g is suggested by BIS-1893 (2016) for Jammu. In the present study, we used bedrock PGA 0.41 g for safe design purposes considering the maximum credible earthquake scenario (Ansari et al. 2022c). The equivalent linear ground response analysis used in this study was done with the premise that the site is stacked horizontally for all frequency components. Although the comparable linear technique is quick and efficient, it is always an approximate estimate of soil non-linear behavior. The damping versus shear strain curves and modulus reduction curves are used to represent the soil parameters of each soil layer. Seed and Sun (1989) and Seed and Idriss (1970) for clays and sands have employed shear modulus reduction curves (G/G_{max}) based on the shear strain to define

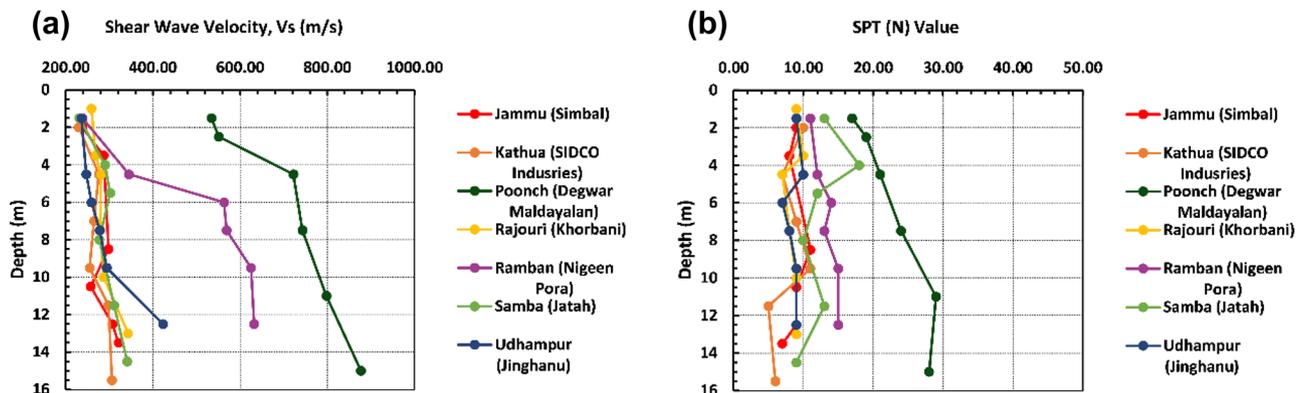


Fig. 5 Depth-wise variation of a SPT (N) value and b shear wave velocity (V_s) for benchmark locations in the study area

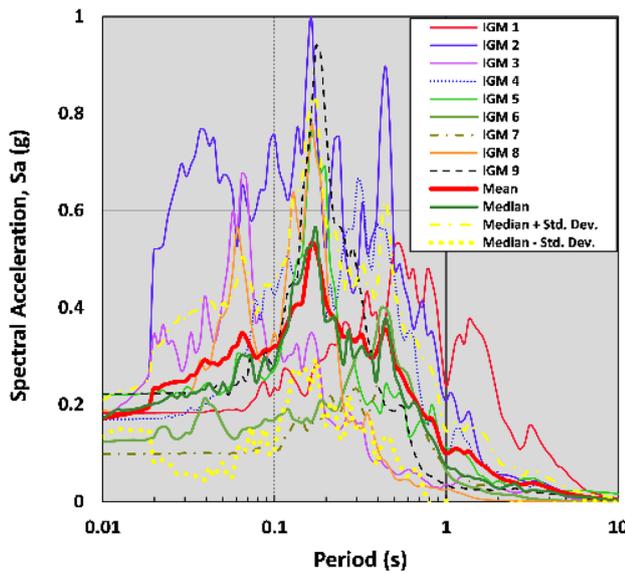


Fig. 6 5% damped response spectra of selected input bedrock motions recorded at Himalayan seismic stations for past earthquake events

the characteristics of the soil using discrete points. For the response analysis, Idriss (1990) modulus reduction curves were used.

Nine seismic stations in the Himalayas recorded the motions (IGM1-IGM9) for the 1991 Uttarkashi earthquake, 1995 Chamba earthquake, 1999 Chamoli earthquake, 2010 South Hindukush, and the most recent 2013 Jammu and Kashmir earthquake. All these past earthquake events triggered the Jammu region JR. Among all nine input motions, the 1991 Uttarkashi and 1999 Chamoli earthquakes are very strong. In a way to consider the effect of both the strong and weak nature of motions, the mean value of PGA is preferred. As shown in Fig. 6, the maximum PGA of the mean spectra of these input motions is 0.52 g.

Based on average shear wave velocity at 30 m depth (V_{s30}), local geology and topography, complete JR is divided into five different classes, class A, class B, class C, class D, and class E. Few sites in the Kishtwar area, in the northwestern part of JR, have hard rock and V_{s30} more than 825 m/s; hence, they are classified as class A. Sites in Kishtwar, northern Reasi, Ramban, and Poonch that exhibit having granite rock at shallow depth are classified as class B, with V_{s30} ranging from 734 to 820 m/s. All locations in Doda, northwestern side of Jammu, Rajouri, and Poonch show dense gravely sands, and are kept in class C for which V_{s30} ranges between 603 to 723 m/s. Most of the sites in southern areas like Jammu, Samba, Kathua, and the central part of Rajouri fall in class D and class E due to sandy deposits. V_{s30} fluctuates between 320 and 587 m/s for class D and 185 to 316 m/s for class E, respectively. Due to younger sedimentary formation, areas like Kunjwani, Rehari Colony

in Jammu, and Katli and Salor in Kathua have an average shear wave velocity of 208 m/s. Table 2 shows the results of the statistical analysis used to determine the disparity of shear wave velocity for JR.

Figure 7 shows the comparison of spectral acceleration, Fourier amplitude ratio, and amplification factor for all these five site classes. At 0.3-s time period, spectral acceleration for class A is 1.56 g, which is highest among all sites taken under consideration during geophysical testing. Fourier amplitude ratio (FAR) is determined by taking the ratio of Fourier amplitude spectra of surface motion and Fourier amplitude spectra of input bedrock motion. Class E has the lowest FAR of 2.75 at 8.5 Hz for all locations. The spectral acceleration computed at the surface for any motion at bedrock during the seismic event determines the amplification ratio (AR).

As one move towards site classes with lower shear wave velocity, the peaks of the amplification factor appear to shift towards a higher period. In general, the amplification factor increases with increasing period length, peaks at the lowest period, and then declines with increasing period length. In the southern section of Jammu, the amplification factor for rock sites (class A) is larger than that for alluvium sites (class E). The FAR plot demonstrates that alluvium sites have a maximum peak at lower frequencies, whereas rocky sites have a higher peak at higher frequencies. Over places with a higher shear wave velocity for a shorter period of time, the amplification is greater. For places with lesser shear wave velocity over a long period of time, the amplification is maximum.

For complete JR, the average trend for these parameters is highlighted using a black-dotted line which satisfies the selected boundary condition of input bedrock motions. The graphical values for these black-dotted lines act as a preliminary database to assess the dynamic behaviors of foundation soil in JR. In general, analysis of soil deposits needed for localized construction projects can employ the general trend plot at the initial stages. But site-specific projects need to follow the specific curves provided for various classes as per characterization and microzonation.

Table 2 Average shear wave velocity (V_{s30})-based statistical parameters for site classification in the Jammu Region

Parameters	Zone A	Zone B	Zone C	Zone D	Zone E
Minimum	821	734	603	320	201
Maximum	935	818	723	587	316
Range	114	84	120	267	115
Sample size	25	62	34	87	34
Mean	857.66	781.79	665.22	445.55	249.63
Median	849.77	785.70	671.27	433.72	251.64
Std. dev	29.6258	18.26	34.09	83.69	28.53

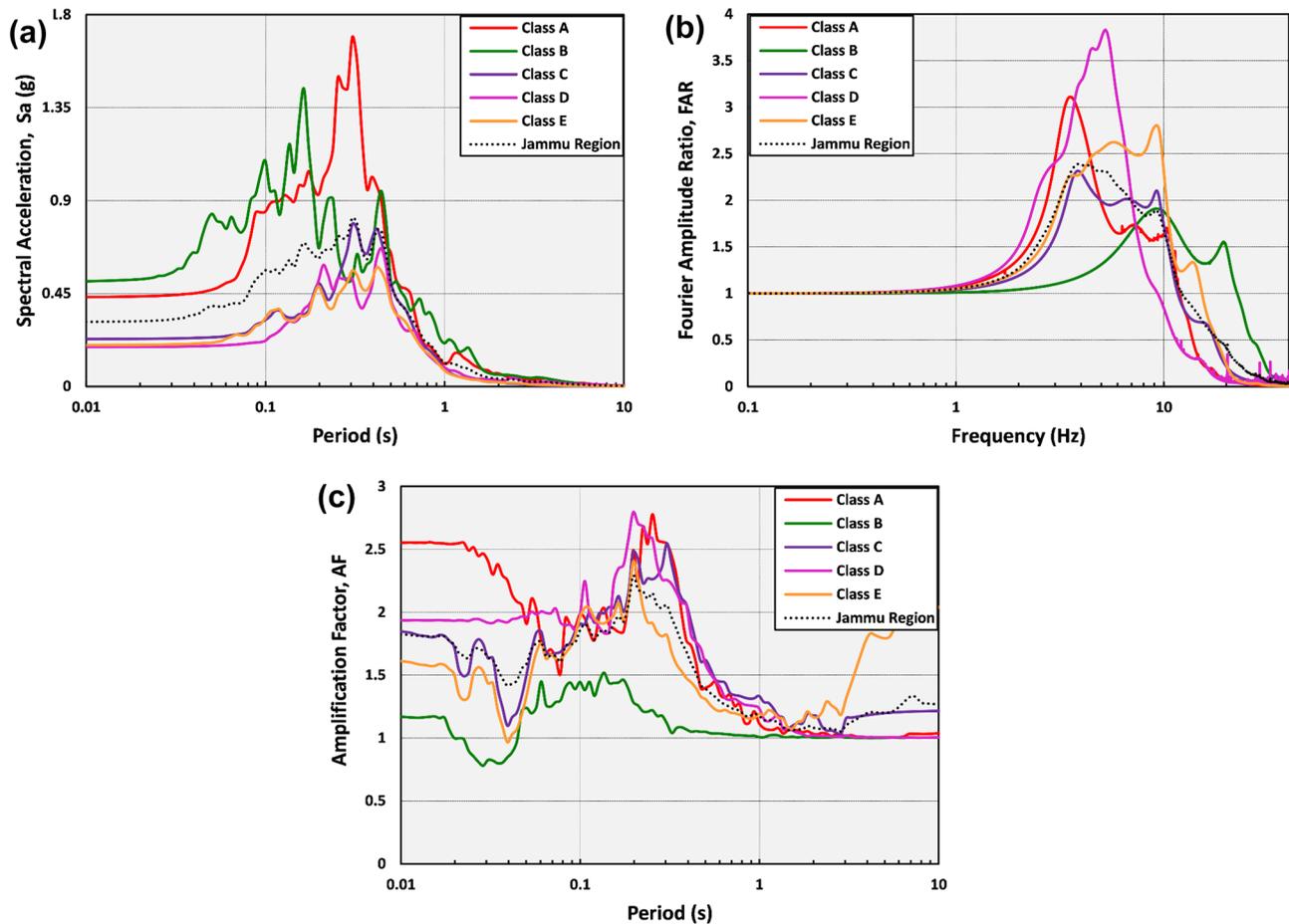


Fig. 7 **a** Spectral acceleration, **b** Fourier amplitude ratio, and **c** amplification factor for different site classes in the Jammu Region, based on the shear wave velocity measured during geophysical testing

The spectral acceleration peaks are maximum for the rocky sites in the northern region as compared to alluvium sites in the southern region covered by Samba, Kathua, and south-eastern parts of Jammu. It has been noted that surface peak ground acceleration (PGA_{surface}) ranges between 0.13 to 0.55 g. The rocky sites in the eastern part of Kishtwar, Poonch, and Ramban on the northern side present $PGA > 0.3$ g. Due to young sediments and alluvium deposits near the Tawi River and Ravi River, maximum sites in Jammu, Samba, Kathua, and the central part of Udhampur exhibit very low surface PGA, as shown in Fig. 8. A maximum surface PGA of 0.56 g was reported at Siksha Niketan School at Jeevan Nagar and Govt. Degree College at Bishnah in Jammu. The surface PGA illustrated in Fig. 8 is used as an input parameter to calculate Cyclic Stress Ratio (CSR) while doing a liquefaction hazard assessment.

Methodology

The earthquake-induced liquefaction leads to create catastrophic hazard potential for life killing and property damages. To overcome such natural disasters and associated failure risks, a liquefaction hazard assessment for an area located in a seismically active region is needed. The most commonly used field testing-based approaches for getting undisturbed soil samples for liquefaction hazard study are standard penetration test (SPT), cone penetration test (CPT), and seismic tests to measure the shear wave velocity of soil deposits. The first method evolved based on the concept of applied stress and resistance offered by subsurface soil layers for SPT tests (Seed and Idriss 1971). Robertson and Campanella (1985) were the first to suggest a CPT-related liquefaction model. Idriss and Boulanger (2008) established the liquefaction analysis methodology, and the expression for r_d was developed from

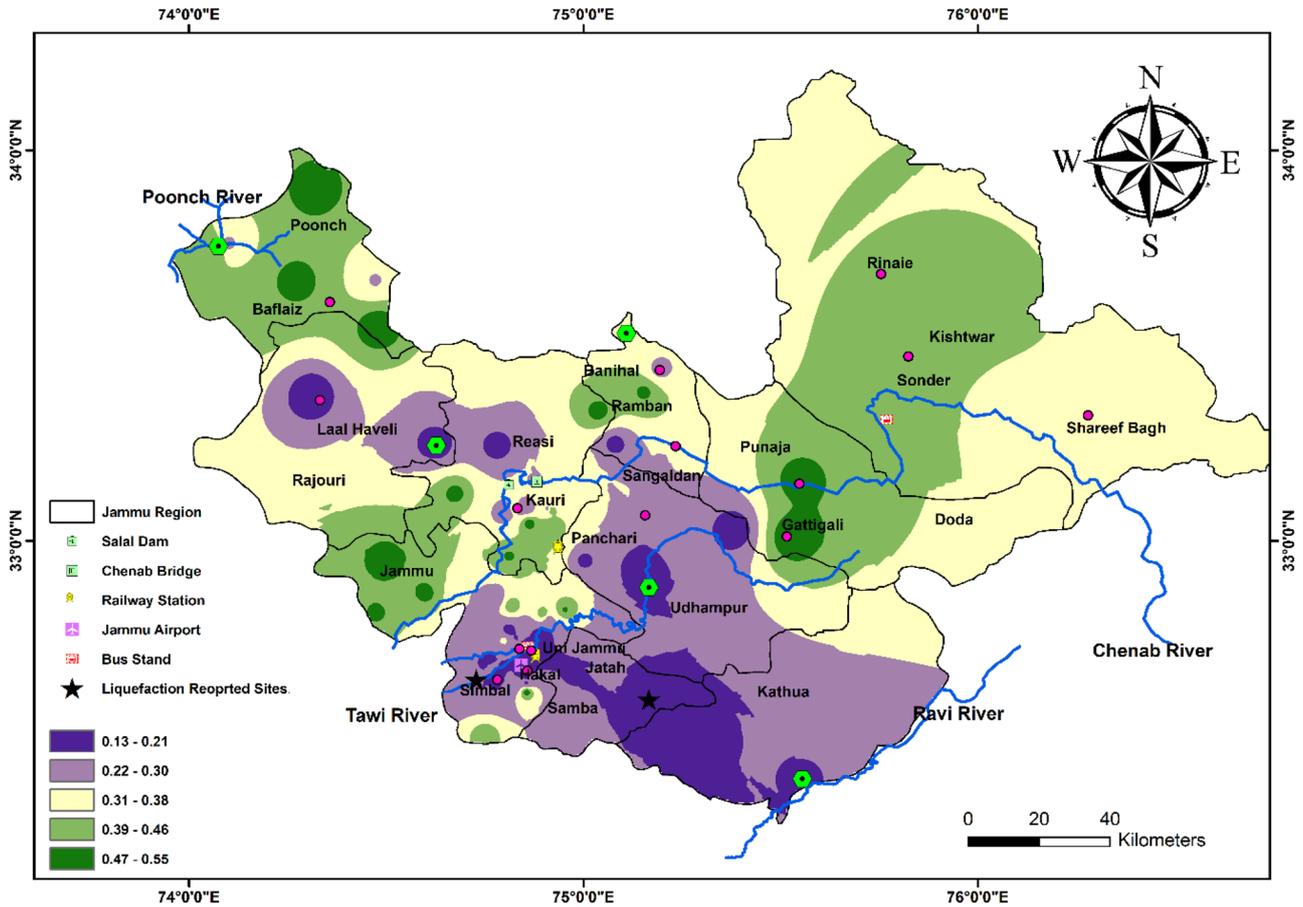


Fig. 8 Spatial distribution of surface peak ground acceleration ($PGA_{surface}$) values for Jammu Region using 1D equivalent linear seismic response analysis

site response investigations by Boulanger and Idriss (2014). Using a maximum likelihood algorithm and an updated case history database, Boulanger and Idriss (2014) proposed probabilistic CPT-based liquefaction triggering the procedure for cohesionless soils. Several studies have significantly improved and altered the SPT-based approach, as the number of field liquefaction case histories using SPT data has grown (Seed and Peacock 1971; Seed and Idriss 1981; Iwasaki et al. 1982; Idriss 1999; Youd et al. 2001; Boulanger and Idriss 2004, 2012; Cetin et al. 2004; Idriss and Boulanger 2006, 2010). The sites having gravelly soils, cobbles even boulders, and boring becomes difficult for SPT and CPT methods. In such cases, the shear wave velocity (V_s)-based method is adopted for site characterization. The V_s is a fundamental characteristic of soil material that is directly linked with shear modulus and is used to predict dynamic soil behavior (Kramer 2000). The liquefaction triggering potential may be calculated using existing correlations and in situ V_s measurements. The shear wave velocity-based approach was used by several researchers to analyze the possibility of soil liquefaction (Lin et al. 2004; Beroya et al. 2009; Karastathis et al. 2010; Castellaro et al. 2015). Qualitative information on subsurface conditions

was acquired through shear wave velocity-based frequency measurements to generate a hybrid hazard map for zonation of liquefaction sites (Huang and Tseng 2002; Beroya et al. 2009; Satyam and Priyadarsini 2021).

Based on V_s , a relationship to assess the cyclic resistance of subsurface strata was created by considering liquefaction case histories from 20 earthquakes and 193 liquefaction and non-liquefaction case histories throughout the world (Andrus and Stokoe 1997). For Andrus and Stokoe (2000) method, cyclic loading due to earthquake, overburden stress corrected shear wave velocity, and soil resistance against liquefaction are the main parts to calculate the F_s for a site susceptible to liquefaction during strong seismic waves. Andrus et al. (2004) adjusted this relationship by introducing a correction factor for cemented and old soil deposits. In this study, the most recent technique suggested for SPT (Boulanger and Idriss 2014) and shear wave velocity (Andrus and Stokoe 2000; Andrus et al. 2004) is used to assess the liquefaction hazard in the study area.

The factor of safety (F_s) is calculated by taking the ratio of cyclic stress ratio (CSR) and cyclic resistance ratio (CRR).

The CSR depends on the surface PGA and can be calculated as follows:

$$CSR = 0.65 \cdot \frac{\sigma_v}{\sigma'_v} \cdot \frac{a_{max}}{g} \cdot r_d \tag{2}$$

In the above Eq. (2), σ_v is the vertical total stress, a_{max} is the maximum $PGA_{surface}$, and r_d is a shear stress reduction factor, defining the dynamic response of soil deposits. The cyclic resistance ratio (CRR) is associated with the SPT (N) value, which is corrected for overburden stress, delivered energy, rod diameter, energy ratio, and type of sampler (Boulanger and Idriss 2014). Duration of ground shaking is also one of the major factors to be considered in terms of magnitude scaling. The empirical equation to calculate CRR is given as follows:

$$CRR_{M,\sigma'_v} = CRR_{M=7.5,\sigma'_v=1atm} \cdot MSF \cdot K_\sigma \cdot K_\alpha \tag{3}$$

Here, in this Eq. (3), MSF is a magnitude scaling factor, K_σ is overburden correction factor, and, K_α is the static shear stress correction factor. The correlation for $CRR_{M=7.5,\sigma'_v=1atm}$ is as follows,

$$CRR_{M=7.5,\sigma'_v=1atm} = \exp \left\{ \frac{(N_1)_{60cs}}{14.1} + \left[\frac{(N_1)_{60cs}}{126} \right]^2 - \left[\frac{(N_1)_{60cs}}{23.6} \right]^3 + \left[\frac{(N_1)_{60cs}}{25.4} \right]^4 - 2.8 \right\} \tag{4}$$

where $(N_1)_{60cs}$ is the equivalent clean sand value for cohesionless soils. The MSF can be estimated using the following Eq. (5).

$$MSF = 6.9 \cdot \exp \left\{ \frac{-M}{4} - 0.058 \right\} \leq 1.8 \tag{5}$$

According to Andrus and Stokoe (2000) method, for shear wave velocity–based evaluation of liquefaction hazard, CRR can be calculated using Eq. (6), as presented below.

$$CRR = \left\{ a \left[\frac{K_c V_{s1}}{100} \right]^2 + b \left(\frac{1}{V_{s1}^* - K_c V_{s1}} - \frac{1}{V_{s1}^*} \right) \right\} \cdot MSF \tag{6}$$

In the above Eq. (6), K_c is the correction factor considered for the high values of overburden stress–corrected shear wave velocity (V_{s1}) due to cementation and aging, ranging between 0.6 to 0.8 (Ohta and Goto 1978; Robertson et al. 1992; Rollins et al. 1998). The value of V_{s1}^* varies between 200 and 215 m/s, based on a percentage of fine content (FC). The V_{s1}^* and FC are related as follows:

$$\begin{aligned} V_{s1}^* &= 215 \text{ m/s, for sands with } FC \leq 5\% \\ V_{s1}^* &= 215 - 0.5(FC - 5) \text{ m/s, for sands with } 5\% < FC < 35\% \\ V_{s1}^* &= 200 \text{ m/s, for sands with } FC \geq 35\% \end{aligned} \tag{7}$$

For older soil deposits, V_{s1} is corrected for an equivalent young, clean soil as follows:

$$(V_{s1})_{csa1} = K_{a1} \cdot K_{cs} \cdot V_{s1} \tag{8}$$

where K_{a1} is an age factor and is considered equal to 1.0 for all Holocene soil deposits (Andrus and Stokoe 2000). The K_{cs} is FC correction factor which can be determined as follows (Juang and Jiang 2000; Juang et al. 2002),

$$\begin{aligned} K_{cs} &= 1.0, \text{ for } FC \leq 5\% \\ K_{cs} &= 1 + (FC - 5)T, \text{ for } 5\% < FC < 35\% \\ K_{cs} &= 1 + 30T, \text{ for } FC \geq 35\% \end{aligned} \tag{9}$$

where,

$$T = 0.009 - 0.0109 (V_{s1}/100) + 0.0038 (V_{s1}/100)^2 \tag{10}$$

Liquefaction potential index (LPI)

The F_s is insufficient for evaluating liquefaction hazards (Toprak and Holzer 2003). Hence, the depth and thickness of layers susceptible to liquefaction are considered to understand the overall damage of any borehole. The liquefaction potential index (LPI) considers both the geometrical parameter of the liquefiable layer and the associated F_s (Iwasaki 1978; Iwasaki et al. 1982). The LPI map for the Kashmir valley was proposed based on SPT-based method, which suggests that maximum boreholes in Baramulla and Kupwara demonstrate very high LPI (Dar and Dubey 2015; Khan and Shah 2016; Sana and Nath 2016; Zahoor et al. 2019). The site condition for different values of LPI and, the required plan of action for liquefaction mitigation is mentioned in Table 3.

The LPI can be determined as follows:

$$LPI = \int_0^{20} F(z) \cdot W(z) dz \tag{11}$$

Table 3 Likelihood of liquefaction at different probability (Iwasaki 1978; Iwasaki et al. 1982)

Liquefaction potential index (LPI)	Description	Further requirement
LPI > 15	Very high chances of liquefaction	A thorough examination, also, countermeasures are required
5 < LPI ≤ 15	High chances of liquefaction	In the case of structures, a detailed study is required. In most cases, a liquefaction countermeasure is important
0 < LPI ≤ 5	Low chances of liquefaction	A more thorough study is required, particularly for infrastructure projects
LPI = 0	Very low chances of liquefaction	A thorough examination is not required

$$\begin{aligned}
 F(z) &= 1 - F_s, \text{ for } F_s < 1.0 \\
 F(z) &= 0, \text{ for } F_s \geq 1.0 \\
 W(z) &= 10 - 0.5z, \text{ for } z < 20 \text{ m.} \\
 W(z) &= 0, \text{ for } z > 20 \text{ m}
 \end{aligned}
 \tag{12}$$

Probability of liquefaction (P_L)

Based on the concept of LPI, the probability of liquefaction (P_L) for any site can be estimated using Eq. (13), proposed by Juang et al. 2002. Table 4 presents the different states for the site under investigation based on the calculated probability of liquefaction.

$$P_L = \frac{1}{1 + \left(\frac{F_s}{0.96}\right)^{4.5}}
 \tag{13}$$

Earthquake-induced liquefaction hazard investigation for the study area

Based on SPT (Boulanger and Idriss 2014), data collected from geotechnical consultancies and shear wave velocity (Andrus and Stokoe 2000; Andrus et al. 2004) estimated from multichannel analysis of surface waves (MASW) during field testing, the comprehensive liquefaction hazard assessment of the JR was carried out. Based on the calculated values of F_s , three distinct categories are fixed to define the potential liquefaction hazard for a particular site. The sites with $F_s < 1.0$ are vulnerable to severe liquefaction, whereas sites with F_s between 1.0 and 1.2 are likely

Table 4 Liquefaction risk assessment based on probability of liquefaction (Chen and Juang 2000; Juang et al. 2002)

Probability of liquefaction (P_L)	Description
$P_L \geq 0.85$	It is almost sure that site will liquefy
$0.65 \leq P_L < 0.85$	Likely to liquefy
$0.35 \leq P_L < 0.65$	Equal possibility of liquefaction or no liquefaction
$0.15 \leq P_L < 0.35$	Unlikely to liquefy
$P_L < 0.15$	It is almost sure that site will not liquefy

to liquefy. Sites with $F_s > 1.2$ are safe and not vulnerable to liquefaction. Table 5 demonstrates typical analytical findings for determining the F_s against liquefaction at benchmark sites using both methodologies. The areas on the northeastern side like Rinaie, Shareef Bagh, Sonder in Kishtwar, and Gattigali and Punaja in Doda are not susceptible to liquefaction, as shown in Fig. 9a. In Gandhi Nagar, Talab Tillo, and Hakal in Jammu, along with several localities near the Tawi River’s bank including Simbal, Ram Bagh, and Jammu University, and eastern sections of Rajouri such as Laal Haveli and Jamia Masjid, the liquefaction hazard is severe. Samba and Kathua have a thick layer of young sedimentary formations with uniformly graded soils showing highly susceptible to liquefaction. Central portions of Udhampur, such as Jinghanu and Panchari, have a sand layer up to 4 m thick, indicating that they are expected to liquefy. Bafflaiz, Morha near Mughal Road in Poonch, and Kauri and Bakkal village near Chenab bridge in Reasi exhibit exceptionally high F_s against liquefaction, due to gravelly sand with high SPT (N) values. The increase in liquefaction resistance over time might be due to the deformation or compression of soil particles into more stable arrangements, as well as a higher degree of consolidation. The maps presented in Fig. 9b, c show the liquefaction hazard zonation based on the F_s values determined using the methods suggested by Andrus and Stokoe (2000) and Andrus et al. 2004, respectively. Due to rock near the surface or at shallow depth, liquefaction threat is low in most portions of the eastern and central regions, according to these two maps: Sangaldan, Chachihal, and Banihal in Ramban, which are located in the northern part of the study area, have a F_s against liquefaction more than 1.2.

Using the findings of both V_s - and SPT-based techniques, an integrated liquefaction hazard map of the study area is also presented and illustrated in Fig. 10. As per this map, Banhore, Sawan Chak, Balour, and Talhar like areas near the bank of the Ravi River in the southern region have extremely low values of SPT (N) and V_s , making them especially vulnerable to liquefaction. Liquefaction is not occurring in the eastern and western parts of the JR which has high shear wave velocities and also not occurring in the central portion because of dense sand. The areas like Babliana, Mehmoodpur, Batna, Khan Pora, and Sawalkot is likely to liquefy as F_s values vary between 1.0 and 1.2.

The LPI of any site offers a better understanding of the borehole related to liquefaction. The determined F_s values at

Table 5 Liquefaction analysis for benchmark locations in the study area

Depth (m)	Total stress σ_v (t/m ²)	SPT-based method						V_s -based method						LPI	LPI of borehole	
		$(N_1)_{60}$	$(N_1)_{60cs}$	r_d	CSR	CRR	F_s	V_{s1}	r_d	CSR	Method 1		Method 2			
											CRR	F_s	CRR			F_s
Jammu (Simbal)																
2.00	3.20	14.10	19.60	0.99	0.36	0.22	0.62	333.20	0.98	0.36	0.21	0.58	0.25	0.69	3.44	15.79
3.50	5.60	13.37	18.88	0.98	0.36	0.21	0.60	401.80	0.97	0.35	0.33	0.92	0.32	0.91	3.29	
8.50	14.10	15.35	20.88	0.92	0.32	0.24	0.75	344.48	0.93	0.32	0.23	0.71	0.20	0.63	2.44	
10.50	17.70	12.38	17.92	0.89	0.30	0.19	0.64	279.00	0.89	0.30	0.12	0.41	0.23	0.78	2.70	
12.50	21.50	11.07	16.61	0.86	0.28	0.17	0.62	315.19	0.84	0.27	0.18	0.66	0.19	0.70	2.43	
13.50	23.40	8.21	13.74	0.84	0.27	0.15	0.54	321.81	0.81	0.26	0.19	0.73	0.25	0.96	1.50	
Kathua (SIDCO Industries)																
2.00	3.20	15.66	21.17	0.99	0.36	0.24	0.68	322.00	0.98	0.36	0.19	0.53	0.18	0.20	4.20	15.70
4.50	7.20	11.70	17.20	0.97	0.35	0.19	0.55	382.88	0.97	0.35	0.29	0.83	0.27	0.77	1.28	
7.00	11.45	14.09	19.61	0.94	0.33	0.22	0.68	324.46	0.95	0.33	0.20	0.59	0.22	0.67	2.68	
9.50	15.95	15.98	21.53	0.90	0.30	0.24	0.79	284.54	0.92	0.31	0.13	0.42	0.25	0.81	4.04	
11.50	19.75	6.42	11.94	0.87	0.29	0.14	0.47	312.68	0.87	0.28	0.18	0.62	0.17	0.62	1.61	
15.50	27.35	6.43	11.97	0.82	0.26	0.13	0.51	293.29	0.76	0.24	0.15	0.61	0.15	0.63	1.89	
Poonch (Degwar Maldayalan)																
1.50	3.15	26.63	32.12	0.97	0.63	0.73	1.15	747.60	0.99	0.63	-	NL	-	NL	0.01	0.05
2.50	5.25	31.74	37.28	0.99	0.62	-	NL	760.88	0.98	0.62	-	NL	-	NL	0.00	
4.50	9.45	31.17	36.71	0.97	0.61	-	NL	860.77	0.97	0.61	-	NL	-	NL	0.00	
7.50	15.75	30.84	36.34	0.93	0.59	-	NL	779.61	0.94	0.60	-	NL	-	NL	0.00	
11.00	23.10	30.77	36.28	0.88	0.56	-	NL	708.42	0.88	0.56	-	NL	-	NL	0.00	
Rajouri (Khorbani)																
1.00	1.60	14.10	19.61	0.98	0.28	0.22	0.80	362.60	0.99	0.28	0.26	0.94	0.25	0.89	0.85	4.42
3.50	5.60	16.71	22.20	0.98	0.27	0.26	0.97	376.60	0.97	0.27	0.28	1.05	0.29	1.07	0.31	
4.50	7.20	12.43	17.92	0.97	0.27	0.20	0.76	389.82	0.97	0.27	0.31	1.14	-	NL	0.89	
7.50	12.00	13.92	19.43	0.93	0.26	0.22	0.86	340.64	0.94	0.26	0.22	0.85	0.21	0.81	0.91	
10.00	16.25	13.29	18.82	0.90	0.24	0.21	0.85	322.78	0.91	0.25	0.19	0.78	0.18	0.72	0.76	
Ramban (Nigeen Pora)																
1.50	2.70	17.23	22.75	0.95	0.23	0.27	1.17	333.20	0.99	0.23	0.21	0.90	0.22	0.96	0.01	0.01
4.50	8.40	18.88	24.42	0.97	0.22	-	NL	436.57	0.97	0.22	-	NL	-	NL	0.00	
6.00	11.55	19.62	25.16	0.95	0.21	-	NL	652.28	0.95	0.21	-	NL	-	NL	0.00	
7.50	14.70	17.88	23.42	0.93	0.20	-	NL	617.70	0.94	0.20	-	NL	-	NL	0.00	
9.50	18.90	18.06	23.59	0.90	0.19	-	NL	634.74	0.92	0.19	-	NL	-	NL	0.00	
12.50	25.20	15.53	21.08	0.86	0.18	-	NL	595.34	0.84	0.17	-	NL	-	NL	0.00	
Samba (Jatah)																
1.50	2.40	20.36	25.88	0.96	0.36	0.35	0.96	323.40	0.99	0.36	0.19	0.54	0.19	0.53	4.28	9.34
4.00	6.40	30.07	35.59	0.97	0.35	-	NL	406.00	0.97	0.35	0.34	0.95	0.33	0.94	0.40	
5.50	8.95	21.30	26.84	0.96	0.34	0.38	1.12	394.05	0.96	0.34	0.31	0.92	0.32	0.94	0.56	
8.00	13.45	15.81	21.34	0.92	0.31	0.24	0.78	322.39	0.94	0.32	0.19	0.61	0.21	0.65	2.36	
11.50	20.10	16.36	21.90	0.87	0.28	0.24	0.85	322.95	0.87	0.28	0.19	0.70	0.21	0.75	1.29	
14.50	25.80	9.88	15.41	0.83	0.26	0.16	0.61	330.74	0.79	0.25	0.21	0.84	0.27	1.08	0.45	
Udhampur (Jinghanu)																
1.50	2.48	14.10	19.61	0.97	0.26	0.22	0.85	330.40	0.99	0.26	0.20	0.78	0.21	0.81	1.40	4.29
4.50	7.28	16.71	22.22	0.97	0.26	0.26	0.99	340.32	0.97	0.26	0.22	0.83	0.22	0.85	0.17	
6.00	9.90	11.70	17.21	0.95	0.25	0.19	0.78	327.74	0.95	0.25	0.20	0.79	0.26	1.04	1.05	
7.50	12.69	12.96	18.47	0.93	0.24	0.21	0.87	327.53	0.94	0.24	0.20	0.83	0.23	0.96	0.32	
9.50	16.37	12.67	18.20	0.90	0.22	0.20	0.88	322.93	0.92	0.23	0.19	0.84	0.21	0.91	0.66	
12.50	21.77	10.91	16.44	0.86	0.21	0.17	0.82	431.09	0.84	0.21	-	NL	-	NL	0.69	

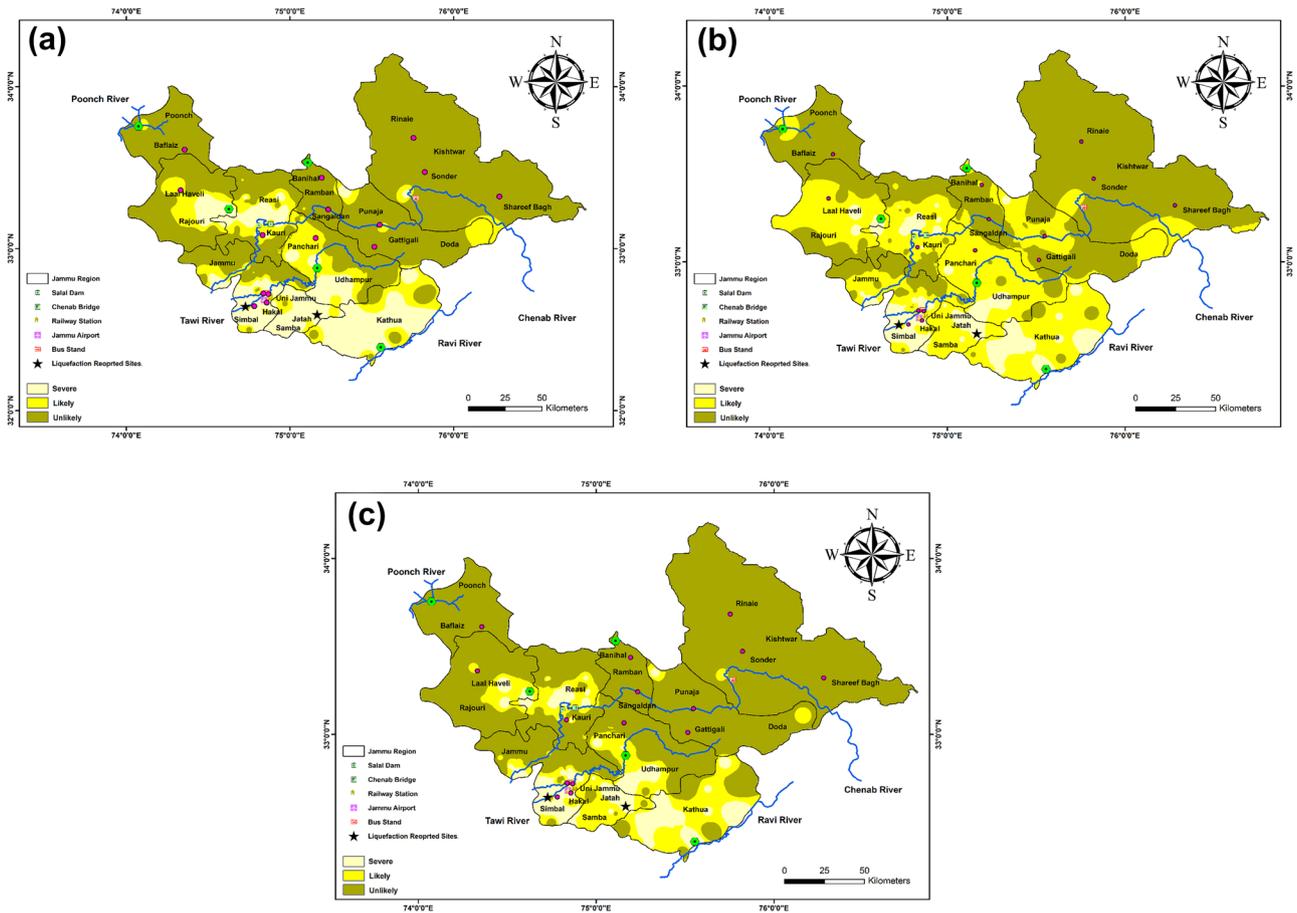


Fig. 9 Liquefaction hazard assessment of Jammu Region using **a** SPT-based method (Boulanger and Idriss 2014), **b** shear wave velocity (V_s)-based method proposed by Andrus and Stokoe 2000, and **c** shear wave velocity (V_s)-based method proposed by Andrus et al. 2004

different depths and thickness of layering for each borehole used to calculate the LPI for the sites under study. According to Iwasaki et al.'s (1982) method, the whole study area is classified into four different zones based on LPI values, as shown in Fig. 11. Based on LPI, boreholes near the bank of Tawi River and Ravi River in southern districts like Jammu, Samba, and Kathua have a very high liquefaction potential due to high water tables. The Simbal village in Jammu and SIDCO industrial area in Kathua show $LPI > 15$. The borehole at Jatah in the Samba district where sand blows were observed during the field survey fall in a high liquefaction potential zone. The maximum of the boreholes in Ramban, Rajouri, and Poonch have a 3–5-m gravel layer exhibit very low LPI, and are not vulnerable to liquefaction. The LPI for boreholes in Reasi and Udhampur ranges from 4.15 to 12.34, indicating a low to high liquefaction potential. The probability of liquefaction (P_L) suggests the likelihood of occurrence of liquefaction features for any site in a seismically active region based on the F_s against liquefaction (Juang et al. 2002). As shown in Fig. 12, the maximum portion

in the northern part of the JR demonstrate $P_L < 0.42$. The western portion of Jammu, Udhampur, and Kathua are likely to liquefy where P_L varies between 0.65 and 0.85. As P_L is less than 0.1 in Poonch and Doda, all sites are either unlikely to liquefy or will not liquefy. The P_L is very high in regions like Chak Lalushah and Babliana in Jammu, as well as areas near the Ravi River in Kathua due to uniformly graded soil at shallow depth.

There is no published study on liquefaction hazard assessment for the JR. Sana and Nath (2016) evaluated earthquake-induced liquefaction hazards across the whole Kashmir valley if we were looking for a study in and around Jammu. Except for the hills and places to the north of Dal Lake (Illahibagh and Zakura), which have minimal liquefaction susceptibility due to the presence of stiff soils, the majority of the lands have a moderate to extremely high liquefaction potential in Srinagar city (Zahoor et al., 2019). The probability of liquefaction estimated for different cities in the Himalayan region are calculated by different researchers are compared in Table 6.

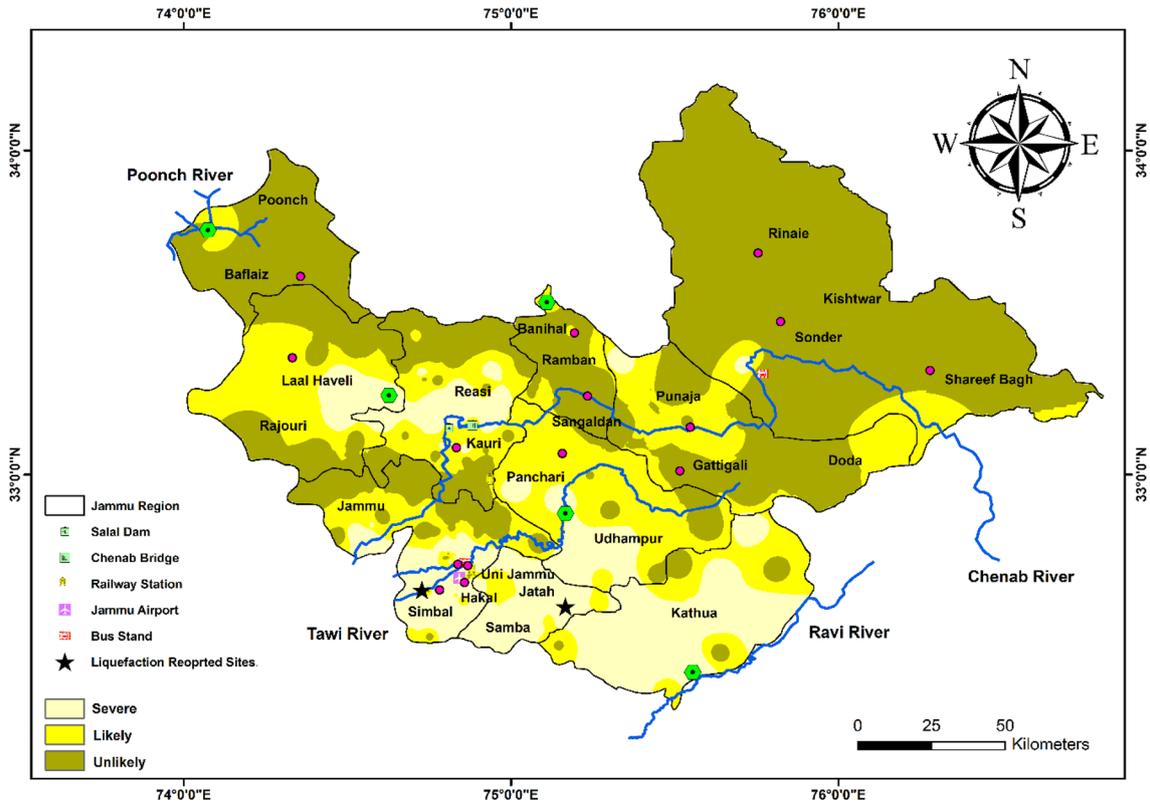


Fig. 10 SPT and shear wave velocity–based integrated liquefaction hazard map of Jammu Region

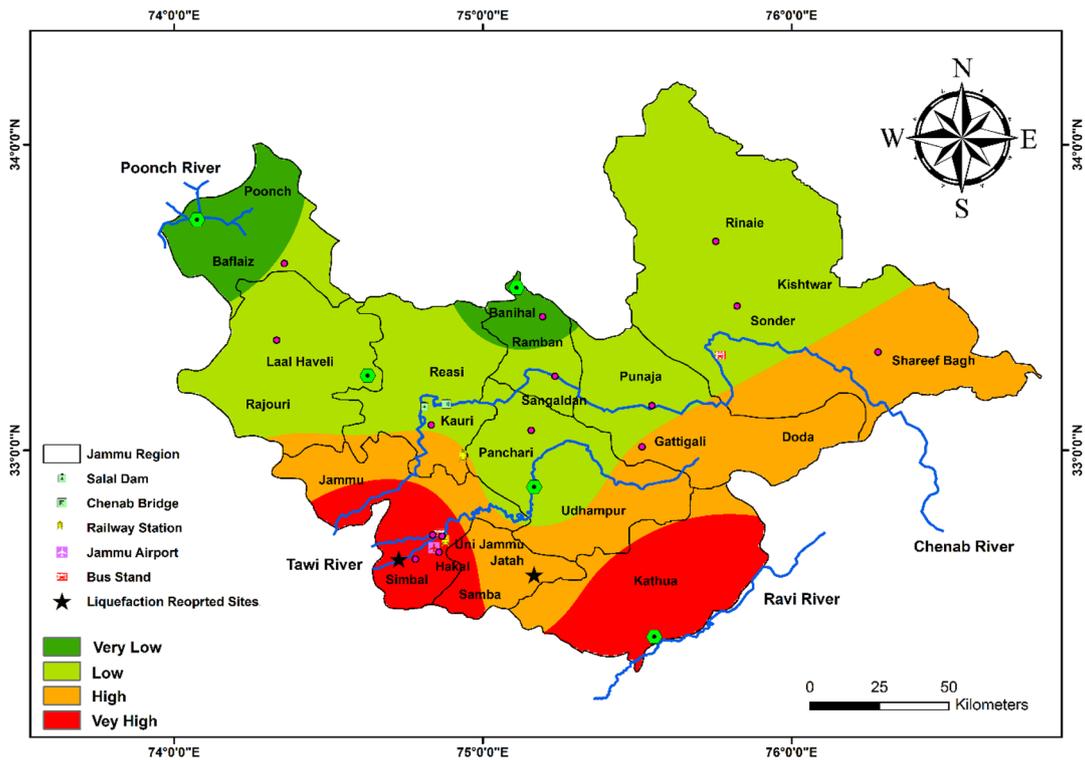


Fig. 11 Liquefaction index (LPI) map of the Jammu region to identify the liquefaction vulnerability of sites subjected to strong ground motion during seismic events, with black stars indicating sites where liquefaction features were documented

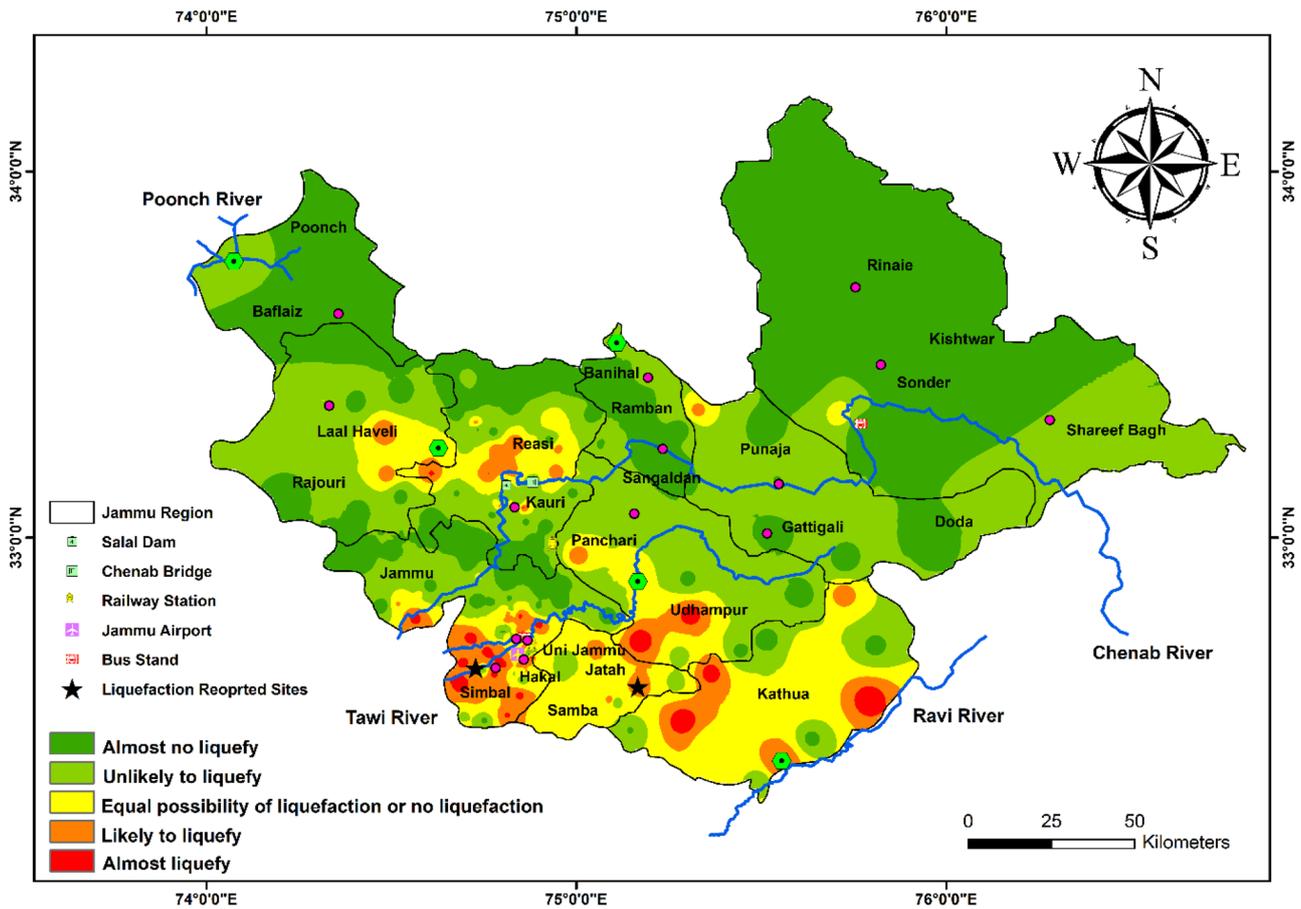


Fig. 12 Spatial distribution of the probability of liquefaction for the Jammu region to check the liquefaction hazard associated with an earthquake

Table 6 Probability of liquefaction (P_L) for the JR compared to previous studies done for various cities in the Himalayas

City name	Probability of liquefaction (P_L)	References
Anantnag	0.78	Sana and Nath (2016)
Baramulla	0.99	
Kupwara	1.00	
Srinagar	0.74	
Srinagar	0.73	Zahoor et al. 2019
Jammu	0.67	Present study
Kathua	0.74	
Poonch	0.09	
Reasi	0.35	

Conclusions

The Jammu Region (JR) in the northwestern Himalayas is jolted by frequent low to high-magnitude earthquakes including the deadliest 2005 Muzaffarabad earthquake and

most recent 2019 Mirpur earthquake. Due to ongoing infrastructure development and urban expansion in such a seismically active area drives to perform liquefaction hazard assessment. In this study, the factor of safety (F_s) against liquefaction is calculated using both SPT- and shear wave velocity (V_s)-based field methods and results are superimposed to generate an integrated map of liquefaction hazards in the JR. The subsurface borehole data was provided by local geotechnical consultancies, and the shear wave velocity was recorded at 243 places during multichannel analysis of surface waves (MASW)-based, geophysical testing using Tromino (Micromed s.p.a. 2009). During the field survey, a 20-m long ground rupture at Simbal near Jammu airport and sand blows near Degh Nala in Jatah were observed as liquefaction evidence of far-field 2019 Mirpur earthquake in Pakistan. The analysis of results showed that some areas are prone to liquefaction using the SPT approach but are not susceptible to liquefaction using the V_s approach. The integrated liquefaction hazard map suggests that liquefaction is severe in the southern portion of the JR where CRR is less than CSR. Maximum parts of Udhampur and Rajouri are

anticipated to liquefaction due to saturated loose to medium dense cohesionless soils. The northern part of Jammu, Reasi, and Ramban together with Kishtwar and Poonch have rocky strata at shallow depth and very high V_s , not susceptible to liquefaction.

The findings from both approaches to determine F_s at different depths and thicknesses of each layer in a borehole used to prepare the map for liquefaction potential index (LPI) for the whole study area. This map illustrates that the central part has low to high, the northwestern part low to very low, and the southern part has a very high LPI. The southern portion of Jammu, Samba, and Kathua located on the Indo-Gangetic Plain have young alluvium and soft sedimentary deposits that reveal a very high probability of liquefaction. The sites in Doda, Poonch, and Kishtwar have very high V_s and rocky strata exhibit a very low probability of liquefaction. The liquefaction hazard maps of the present study can be used for future design and analysis of infrastructures subjected to earthquake risk.

Acknowledgements The authors would like to thank the M/S DMB Pvt. Limited, Space Engineers Consortium Pvt. Limited and, Mount Geotechnical Services Pvt. Limited for providing the SPT data including other geotechnical properties for this study. The authors thank for the technical and logistical assistance offered by the National Institute of Technology Srinagar and the University of Jammu. Prof. Kevin Franke (Brigham Young University, USA) and Prof. Ganesh W Rathod (University of Witwatersrand, South Africa) helped to understand the fundamentals of soil dynamics and liquefaction hazard. The authors appreciate the geotechnical and geological parameters provided by Northern Railways, Konkan Railway Corporation Limited (KRCL), and Ircon International. The authors are also thankful to the Divisional Commissioner Office of Jammu and Kashmir for providing special permission during the COVID-19 pandemic for fieldwork in Jammu and Kashmir.

References

- Ahmad B, Sana H, Alam A (2014) Macroseismic intensity assessment of 1885 Baramulla Earthquake of northwestern Kashmir Himalaya, using the Environmental Seismic Intensity scale (ESI 2007). *Quatern Int* 321:59–64
- Alam A, Ahmad S, Bhat MS, Ahmad B (2015) Tectonic evolution of Kashmir basin in northwest Himalayas. *Geomorphology* 239:114–126
- Andrus RD, Stokoe KH II (2000) Liquefaction resistance of soils from shear-wave velocity. *J Geotech Geoenviron Eng* 126(11):1015–1025
- Andrus RD, Stokoe KH (1997) Liquefaction resistance based on shear wave velocity. Proc., NCEER Workshop on Evaluation of Liquefaction Resistance of Soils, Tech. Rep. NCEER-97, 89–128
- Andrus RD, Stokoe KH, Hsein Juang C (2004) Guide for shear-wave-based liquefaction potential evaluation. *Earthq Spectra* 20(2):285–308
- Ansari A, Rao KS, Jain AK (2021a) Seismic hazard and risk assessment in Maharashtra: a critical review. In: Sitharam, T.G., Kolathayar, S., Sharma, M.L. (Eds), *Seismic hazards and risk*, Lecture Notes in Civil Engineering. Springer, Singapore. pp. 35–45. https://doi.org/10.1007/978-981-15-9976-7_4
- Ansari A, Rao KS, Jain AK (2022a) Damage assessment of tunnels in seismic prone zone during earthquakes: a part of hazard evaluation. In: Sitharam, T.G., Kolathayar, S., Jakka, R. (Eds), *Earthquakes and structures*, Lecture Notes in Civil Engineering. Springer, Singapore. pp. 161–169. https://doi.org/10.1007/978-981-16-5673-6_13
- Ansari A, Rao, KS, Jain AK (2022c) Seismic analysis of shallow tunnels in soil medium. In: Satyanarayana Reddy, C.N.V., Muthukkumaran, K., Vaidya, R. (Eds.), *Stability of slopes and underground excavations*, Lecture Notes in Civil Engineering. Springer, Singapore. pp. 343–352. https://doi.org/10.1007/978-981-16-5601-9_29
- Ansari A, Satake K, Malik JN (2017) Modelling the 2004 Indian Ocean Tsunami to estimate tsunami heights and its amplitude and to study its effects on coastal areas. Proc. of the ERI Earthquake Conference, University of Tokyo, Japan
- Ansari A, Zahoor F, Rao KS, Jain AK (2022b) Deterministic approach for seismic hazard assessment of Jammu Region, Jammu and Kashmir. In *Geo-Congress 2022c: Geophysical and Earthquake Engineering and Soil Dynamics*, GSP(334), 590–598
- Ansari A, Zahoor F, Rao KS, Jain AK (2022d) Seismic hazard assessment studies based on deterministic and probabilistic approaches for the Jammu region, NW Himalayas. *Arab Jo Geosci* 15(11):1–26
- Ansari A, Zahoor F, Rao KS, Jain AK, Riyaz TU (2021b) Seismic vulnerability of residential buildings in Jammu City, Jammu and Kashmir. Proc. of the Indian Geotechnical Conference (IGC), Trichy, India
- Ansari A., Rao KS, Jain AK (2022e) Damage analysis of seismic response of shallow tunnels in Jammu. In: Das BB, Hettiarachchi H, Sahu PK, Nanda S (Eds) *Recent developments in sustainable infrastructure (ICRDSI-2020)—GEO-TRA-ENV-WRM*. Lecture Notes in Civil Engineering, vol 207. Springer, Singapore, pp 611–619 https://doi.org/10.1007/978-981-16-7509-6_47
- Asim KM, Martínez-Álvarez F, Basit A, Iqbal T (2017) Earthquake magnitude prediction in Hindukush region using machine learning techniques. *Nat Hazards* 85(1):471–486
- Avouac JP, Ayoub F, Leprince S, Konca O, Helmlinger DV (2006) The 2005, Mw 7.6 Kashmir earthquake: sub-pixel correlation of ASTER images and seismic waveforms analysis. *Earth Planet Sci Lett* 249(3–4):514–528
- Beroya MAA, Aydin A, Tiglao R, Lasala M (2009) Use of microtremor in liquefaction hazard mapping. *Eng Geol* 107(3–4):140–153
- Bhanja SN, Mukherjee A, Rodell M (2018) Groundwater storage variations in India. In *Groundwater of South Asia*, Springer, Singapore, pp 49–59
- Bilham R, Wallace K (2005) Future Mw>8 earthquakes in the Himalaya: implications from the 26 Dec 2004 Mw=9.0 earthquake on India's eastern plate margin. *Geol Surv India Spec Publ* 85:1–14
- Bonilla LF, Steidl JH, Lindley GT, Tumarkin AG, Archuleta RJ (1997) Site amplification in the San Fernando Valley, California: variability of site-effect estimation using the S-wave, coda, and H/V methods. *Bull Seismol Soc Am* 87(3):710–730
- Boulanger RW, Idriss IM (2004) Evaluating the potential for liquefaction or cyclic failure of silts and clays. Davis, California: Center for Geotechnical Modeling, pp 131
- Boulanger RW, Idriss IM (2012) Probabilistic standard penetration test-based liquefaction-triggering procedure. *J Geotech Geoenviron Eng* 138(10):1185–1195
- Boulanger RW, Idriss IM (2014) CPT and SPT based liquefaction triggering procedures. Report No. UCDC/GM.-14, 1
- Castellaro S, Panzeri R, Mesiti F, Bertello L (2015) A surface seismic approach to liquefaction. *Soil Dyn Earthq Eng* 77:35–46

- Cetin KO, Seed RB, Der Kiureghian A, Tokimatsu K, Harder LF Jr, Kayen RE, Moss RE (2004) Standard penetration test-based probabilistic and deterministic assessment of seismic soil liquefaction potential. *J Geotech Geoenviron Eng* 130(12):1314–1340
- CGWB (2020) Ground water year book 2018–19 Jammu & Kashmir. Central Ground Water Board-North Western Himalayan Region, Ministry of Water Resources, Government of India
- Chen CJ, Juang CH (2000) Calibration of SPT- and CPT-based liquefaction evaluation methods. In: Mayne PW, Hryciw R (Eds) Innovations and applications in geotechnical site characterization. Geotechnical Special Publication 97. ASCE, Reston, pp 49–64
- Dar JA, Dubey RK (2015) Probabilistic seismic hazard analyses (PSHA) and liquefaction susceptibility evaluation of Kashmir Valley, India. *Proc Natl Acad Sci India Sect A* 85(1):177–186
- Ferraro A, Grasso S, Massimino MR (2018) Site effects evaluation in Catania (Italy) by means of 1-D numerical analysis. *Ann Geophys* 61(2):SE224–SE224
- Grasso S, Massimino MR, Sammito MSV (2020) New stress reduction factor for evaluating soil liquefaction in the coastal area of Catania (Italy). *Geosciences* 11(1):12
- Grasso S, Maugeri M (2008) The Seismic Dilatometer Marchetti Test (SDMT) for evaluating liquefaction potential under cyclic loading. In *Geotechnical Earthquake Engineering and Soil Dynamics IV*, pp 1–15
- Gupta H, Gahalaut VK (2014) Seismotectonics and large earthquake generation in the Himalayan region. *Gondwana Res* 25(1):204–213
- Gupta K, Satyam N (2022) Estimation of Arias intensity and peak ground acceleration (PGA) using probabilistic seismic hazard assessment of Uttarakhand state (India). *Arab J Geosci* 15:437. <https://doi.org/10.1007/s12517-022-09733-9>
- Hashash YMA, Groholski DR, Phillips CA, Park D (2008) DEEPSOIL v3.5beta. University of Illinois, U.C., User manual and tutorial
- Huang HC, Tseng YS (2002) Characteristics of soil liquefaction using H/V of microtremors in Yuan-Lin area, Taiwan. *Terr Atmos Ocean Sci* 13(3):325–338
- Idriss IM (1990) Response of soft soil sites during earthquakes. In: *Proceedings of H. Bolton Seed Memorial Symposium*, vol 2, No. 4. University of California, Berkeley
- Idriss IM (1999) An update to the Seed-Idriss simplified procedure for evaluating liquefaction potential. *Proc., TRB Workshop on New Approaches to Liquefaction*, Publ. n. FHWA-RD-99–165, Federal Highway Administration
- Idriss IM, Boulanger RW (2006) Semi-empirical procedures for evaluating liquefaction potential during earthquakes. *Soil Dyn Earthq Eng* 26(2–4):115–130
- Idriss IM, Boulanger RW (2008) Soil liquefaction during earthquakes. *Earthq Eng Res Inst*
- Idriss IM, Boulanger RW (2010) PT-based liquefaction triggering procedures. *Rep UCD/CGM-10* 2:4–13
- Iwasaki T (1978) A practical method for assessing soil liquefaction potential based on case studies at various sites in Japan. In *Proc. Second Int. Conf Microzonation Safer Construct Re Appl* 2:885–896
- Iwasaki T, Tokida KI, Tatsuoka F, Watanabe S, Yasuda S, Sato H (1982) Microzonation for soil liquefaction potential using simplified methods. In *Proceedings of the 3rd international conference on microzonation*, Seattle 3(2):1310–1330
- Jayangondaperumal R, Thakur VC, Suresh N (2008) Liquefaction features of the 2005 Muzaffarabad–Kashmir earthquake and evidence of palaeoearthquakes near Jammu, Kashmir Himalaya. *Curr Sci* 1071–1077
- Jishnu RB, Naik SP, Patra NR, Malik JN (2013) Ground response analysis of Kanpur soil along Indo-Gangetic Plains. *Soil Dyn Earthq Eng* 51:47
- Juang CH, Jiang T (2000) Assessing probabilistic methods for liquefaction potential evaluation. In *Soil dynamics and liquefaction*, pp 148–162
- Juang CH, Jiang T, Andrus RD (2002) Assessing probability-based methods for liquefaction potential evaluation. *J Geotechn Geoenviron Eng* 128(7):580–589
- Karastathis VK, Karmis P, Novikova T, Roumelioti Z, Gerolymatou E, Papanastassiou D, Liakopoulos S, Tsombos P, Papadopoulos GA (2010) The contribution of geophysical techniques to site characterisation and liquefaction risk assessment: case study of Nafplion City, Greece. *J Appl Geophys* 72(3):194–211
- Khan RA, Shah MY (2016) Earthquake induced liquefaction features in the Karewas of Kashmir Valley North-West Himalayas, India: implication to paleoseismicity. *Soil Dyn Earthq Eng* 90:101–111
- Kramer SL (2000) *Geotechnical earthquake engineering*. Prentice Hall, Int Series in Civil Engg and Engg Mech, New Jersey, p 653
- Lin CP, Chang CC, Chang TS (2004) The use of MASW method in the assessment of soil liquefaction potential. *Soil Dyn Earthq Eng* 24(9–10):689–698
- Lister G, Kennett B, Richards S, Forster M (2008) Boudinage of a stretching slablet implicated in earthquakes beneath the Hindu Kush. *Nat Geosci* 1(3):196–201
- Mahajan AK, Mundepi AK, Chauhan N, Jasrotia AS, Rai N, Gachhayat TK (2012) Active seismic and passive microtremor HVSR for assessing site effects in Jammu city, NW Himalaya, India—a case study. *J Appl Geophys* 77:51–62
- Malik JN, Mohanty C (2007) Active tectonic influence on the evolution of drainage and landscape: geomorphic signatures from frontal and hinterland areas along the Northwestern Himalaya. *Ind J Asian Earth Sci* 29(5–6):604–618
- Malik JN, Sahoo AK, Shah AA, Rawat A, Chaturvedi A (2007) Farthest recorded liquefaction around Jammu caused by 8 October 2005 Muzaffarabad earthquake of Mw= 7.6. *Jr Geol Soc India* 69(1):39
- Micromed s.p.a. (2009) *The short Tromino how to*. Ver 1(1):26
- Naik SP, Choudhury B, Garg A (2021) Laboratory investigations of liquefaction mitigation of Ganga sand using stable carbon material: a case study. *Int J Geosynth Ground Eng*. 7:89. <https://doi.org/10.1007/s40891-021-00333-3>
- Naik SP, Mohanty A, Porfido S, Tuttle M, Gwon O, Kim YS (2020) Intensity estimation for the 2001 Bhuj earthquake, India on ESI-07 scale and comparison with historical 16th June 1819 Allah Bund earthquake: a test of ESI-07 application for intraplate earthquakes. *Quatern Int* 536:27–143
- Naik SP, Patra NR (2018) Generation of liquefaction potential map for Kanpur city and Allahabad city of northern India: an attempt for liquefaction hazard assessment. *Geotech Geol Eng* 36(1):293–305
- Nardone L, Maresca R (2011) Shallow velocity structure and site effects at Mt. Vesuvius, Italy, from HVSR and array measurements of ambient vibrations. *Bull Seismol Soc Amer* 101(4):1465–1477
- Ohta Y, Goto N (1978) Empirical shear wave velocity equations in terms of characteristic soil indexes. *Earthquake Eng Struct Dynam* 6(2):167–187
- Pandey SJ, Bhat GM, Puri S, Raina N, Sing Y, Pandita SK, Verma M, Bansal BK, Sutar A (2017) Seismotectonic study of Kishtwar region of Jammu Province using local broadband seismic data. *J Seismolog* 21(3):525–538
- Pandita SK, Haq AU, Bhat GM, Singh Y, Singh A (2021) Identification of active fault topography along the Kishtwar Fault, Jammu and Kashmir, Northwest Himalaya, India. *Environ Earth Sci* 80(4):1–16
- Pandita SK, Singh Y, Bhat GM, Pandey SJ, Singh A, Verma M, Bansal BK (2019) Evidence of active tectonic deformation in Kishtwar

- Area, Jammu and Kashmir, Northwest Himalaya. *India J Geol Soc India* 93(3):331–342
- Papathanassiou G (2008) LPI-based approach for calibrating the severity of liquefaction-induced failures and for assessing the probability of liquefaction surface evidence. *Eng Geol* 96(1–2):94–104
- Park CB, Miller RD, Miur H (2002) Optimum field parameters of an MASW survey. *Japanese Society of Exploration Geophysics Extended Abstracts*
- Park CB, Miller RD, Xia J (1999) Multichannel analysis of surface waves. *Geophysics* 64(3):800–808
- Park CB, Miller RD, Xia J (2001) January. Offset and resolution of dispersion curve in multichannel analysis of surface waves (MASW). In *Symposium on the Application of Geophysics to Engineering and Environmental Problems*, Society of Exploration Geophysicists, SSM4-SSM4
- Pathier E, Fielding EJ, Wright TJ, Walker R, Parsons BE, Hensley S (2006) Displacement field and slip distribution of the 2005 Kashmir earthquake from SAR imagery. *Geophys Res Lett* 33(20)
- Paul H, Priestley K, Powali D, Sharma S, Mitra S, Wanchoo S (2018) Signatures of the existence of frontal and lateral ramp structures near the Kishtwar Window of the Jammu and Kashmir Himalaya: evidence from microseismicity and source mechanisms. *Geochem Geophys Geosyst* 19(9):3097–3114
- Powali D, Sharma S, Mandal R, Mitra S (2020) A reappraisal of the 2005 Kashmir (Mw 7.6) earthquake and its aftershocks: Seismotectonics of NW Himalaya. *Tectonophysics* 789:228501
- Putti SP, Satyam N (2018) Ground response analysis and liquefaction hazard assessment for Vishakhapatnam city. *Innov Infrastruct Solut* 3(1):1–14
- Qadir J, Bhat MS, Alam A, Rashid I (2020) Mapping groundwater potential zones using remote sensing and GIS approach in Jammu Himalaya. *Jammu and Kashmir Geojournal* 85(2):487–504
- Raazia S, Dar AQ (2021) Insights into the hydrogeological framework of the NW Himalayan Karewas (India). *Environ Challenges* 4:100086
- Rai DC, Murty CVR (2006) Effects of the 2005 Muzaffarabad (Kashmir) earthquake on built environment. *Curr Sci* 90(8):1066–1070
- Rao KS, Rathod GW (2014) Seismic microzonation of Indian megacities: a case study of NCR Delhi. *Ind Geotech J* 44(2):132–148
- Rao KS, Satyam DN (2007) Liquefaction studies for seismic microzonation of Delhi region. *Curr Sci* 646–654
- Rathod GW (2011) Seismic hazard assessment and development of attenuation relationship for NCR of Delhi, Ph.D. thesis, Indian Institute of Technology Delhi, New Delhi
- Rix GJ, Lai CG, Orozco, MC, Hebel GL, Roma V (2001) Recent advances in surface wave methods for geotechnical site characterization. In *Proceedings of the international conference on soil mechanics and geotechnical engineering*. AA Balkema Publishers, pp 499–502
- Robertson PK, Campanella RG (1985) Liquefaction potential of sands using the CPT. *J Geotech Eng* 111(3):384–403
- Robertson PK, Woeller DJ, Finn WDL (1992) Seismic cone penetration test for evaluating liquefaction potential under cyclic loading. *Can Geotech J* 29(4):686–695
- Rollins KM, Evans MD, Diehl NB, William DD III (1998) Shear modulus and damping relationships for gravels. *J Geotech Geoenviron Eng* 124(5):396–405
- Sana H (2019) A probabilistic approach to the seismic hazard in Kashmir basin. *NW Himalaya Geosci Lett* 6(1):1–11
- Sana H, Nath SK (2016) Liquefaction potential analysis of the Kashmir valley alluvium, NW Himalaya. *Soil Dyn Earthq Eng* 85:11–18
- Sana H, Nath SK (2017) Seismic source zoning and maximum credible earthquake prognosis of the Greater Kashmir Territory, NW Himalaya. *J Seismolog* 21(2):411–424
- Sana H, Nath SK, Gujral KS (2019) Site response analysis of the Kashmir valley during the 8 October 2005 Kashmir earthquake (Mw 7.6) using a geotechnical dataset. *Bull Eng Geol Env* 78(4):2551–2563
- Satyam DN (2006) Seismic microzonation of Delhi region, Ph.D. thesis. Indian Institute of Technology Delhi, New Delhi, India
- Satyam DN, Rao KS (2008) Seismic site characterization in Delhi region using multi channel analysis of shear wave velocity (MASW) testing. *Electron J Geotech Eng* 13:167–183
- Satyam DN, Rao KS (2014) Liquefaction hazard assessment using SPT and VS for two cities in India. *Indian Geotech J* 44(4):468–479
- Satyam N, Priyadarsini PS (2021) Seismic site characterization and dynamic analysis of pile-supported wharf structure. *Indian Geotech J* 51:211–224. <https://doi.org/10.1007/s40098-020-00482-8>
- Seed HB, Idriss IM (1970) Soil moduli and damping factors for dynamic response analyses. Report EERC 70–10, Earthquake Engineering Research Center, University of California, Berkeley
- Seed HB, Idriss IM (1971) Simplified procedure for evaluating soil liquefaction potential. *J Soil Mech Found Div* 97(9):1249–1273
- Seed HB, Idriss IM (1981) Evaluation of liquefaction potential sand deposits based on observation of performance in previous earthquakes. In *ASCE national convention (MO)*
- Seed HB, Peacock WH (1971) Test procedures for measuring soil liquefaction characteristics. *J Soil Mech Found Div* 97(8):1099–1119
- Seed HB, Sun JI (1989) Implications of site effects in the Mexico City earthquake of Sept. 19, 1985 for earthquake-resistant design criteria in the San Francisco Bay Area of California. University of California, Berkeley, Earthquake Engineering Research Center
- Singh AP, Parmar A, Chopra S (2017) Microtremor study for evaluating the site response characteristics in the Surat City of western India. *Nat Hazards* 89(3):1145–1166
- Singh K (2010) Tectonic evolution of Kishtwar window with respect to the Main Central Thrust, northwest Himalaya, India. *J Asia Earth Sci* 39(3):125–135
- Srinivas GS, Goverdhan K, Narsimhulu CH, Seshunarayana T (2014) Estimation of shearwave velocity in drifts using multichannel analysis of surface wave (MASW) technique—a case study from Jammu & Kashmir, India. *J Geol Soc India* 84(2):174–180
- Thaker TP, Rao KS (2014) Seismic hazard analysis for urban territories: a case study of Ahmedabad region in the state of Gujarat, India. In *Advances in Soil Dynamics and Foundation Engineering*, pp 219–228
- Thaker TP, Rathod GW, Rao KS, Gupta KK (2012) Use of seismotectonic information for the seismic hazard analysis for Surat city, Gujarat, India: deterministic and probabilistic approach. *Pure Appl Geophys* 169(1):37–54
- Tiwari G, Latha GM (2020) Stability analysis and design of stabilization measures for Chenab railway bridge rock slopes. *Bull Eng Geol Env* 79(2):603–627
- Topra S, Holzer TL (2003) Liquefaction potential index: field assessment. *J Geotech Geoenviron Eng* 129(4):315–322
- Trivedi SS, Rao KS, Gupta KK, Rathod GW (2009) Mapping of average shear wave velocity for Ahmedabad soil sites: a case study. *GEO-TIDE, Proceedings of Indian Geotechnical Conference (IGC)*
- Yilmaz Ö, Eser M, Berilgen M (2006) A case study of seismic zonation in municipal areas. *Lead Edge* 25(3):319–330
- Youd TL, Idriss IM, Andrus RD, Arango I, Castro G, Christian JT, Dobry R, Finn WDL, Harder LF, Hynes ME, Ishihara K, Koester JP, Liao SSC, Marcuson W, Martin GR, Mitchell JK, Moriawaki Y, Power MS, Robertson PK, Seed RB, Stokoe KH (2001) Liquefaction resistance of soils: summary report from the 1996 NCEER and 1998 NCEER/NSF workshops on evaluation of liquefaction resistance of soils. *J Geotechn Geoenviron Eng ASCE* 127(10):817–33
- Zahoor F, Rao KS, Banday ZZ, Bhat MA, Farooq M (2019) Liquefaction potential analysis of Srinagar city, Jammu and Kashmir. In *Earthquake Geotechnical Engineering for Protection and*

Development of Environment and Constructions, CRC Press, pp 5807–5814

Zhan Z, Kanamori H (2016) Recurring large deep earthquakes in Hindu Kush driven by a sinking slab. *Geophys Res Lett* 43(14):7433–7441

Springer Nature or its licensor holds exclusive rights to this article under a publishing agreement with the author(s) or other rightsholder(s); author self-archiving of the accepted manuscript version of this article is solely governed by the terms of such publishing agreement and applicable law.